UNIL | Université de Lausanne
Faculté de biologie
et de médecine

Ludwig Institute For Cancer Research

CHUV

Mémoire de maîtrise en médecine

Characterization of tumor reactive CD8 T cells induced by peptide vaccination in melanoma patients

by

Nathalie Rufer

Lausanne, Novembre 2010

Tuteur: Prof. Pedro Romero, Ludwig Institut for Cancer Research

Expert: Prof. Margot Thome Miazza, Dpt of Biochemistry, UNIL

ABSTRACT

Naturally acquired tumor-specific T-cells can be detected in most advanced cancer patients. Yet, they often fail to control or eliminate the disease, in contrast to many virus-specific CD8 T lymphocytes. Therapeutic vaccines aim at inducing and boosting specific T-cells mediated immunity to reduce tumor burden. The properties of CD8 T-cells required for protection from infectious disease and cancer are only partially characterized.

The objectives of this study were to assess effector functions, stage of differentiation and clonotype selection of tumor-reactive T lymphocytes following peptide vaccination in melanoma patients over time. Results were compared to protective viral-specific T-cell responses found in healthy individuals. We also characterized dominant versus low/non dominant T-cell clonotypes with the aim to further understand the *in vivo* function of each set of frequency-based specific T-cells.

Here we developed and applied a novel approach for molecular and functional analysis of single T lymphocytes *ex vivo*. T-cell receptor (TCR) clonotype mapping revealed rapid selection and expansion of co-dominant T-cell clonotypes, which made up the majority of the highly differentiated "effector" T-cells, but only 25% of the less differentiated "effector-memory" cells, mostly composed of non-dominant clonotypes. Moreover, we show that advanced effector cell differentiation was indeed clonotype-dependent. Surprisingly, however, the acquisition of effector functions (cytokine production, killing) was clonotype-independent. Vaccination of melanoma patients with native peptide induced competent effector function in both dominant and non-dominant clonotypes, suggesting that most if not all clonotypes participating in a T-cell response have the potential to develop equal functional competence. In contrast, many T-cells remained poorly functional after vaccination with analog peptide, despite similar clonotype-dependent differentiation. Our findings show that the type of peptide vaccine has a critical influence on the selection and functional activation of the clonotypic T-cell repertoire. They also show that systematic assessment of individual T-cells identifies the cellular basis of immune responses, contributing to the rational development of vaccines.

KEYWORDS

Human, melanoma, vaccination, EBV, CMV, CD8 T-cells, single-cell, differentiation, TCR repertoire, clonotype, gene expression, protein expression, cytolysis, molecular biology

ABBREVIATIONS

IFA, Incomplete Freud's Adjuvant; PBMCs, peripheral blood mononuclear cells; TCR, T-cell receptor; EBV, Epstein-Barr virus; CMV, Cytomegalovirus; EM, effector-memory; EMRA, effector

ACKNOWLEDGEMENTS

We are obligated to the patients and blood donors for their dedicated collaboration in this study, and Pfizer and Coley Pharmaceutical Group for providing CpG PF-3512676/7909. We gratefully acknowledge V. Appay, L. Baitsch, C. Barbey, M. Bruyninx, L. Derré, E. Devevre, P. Guillaume, C. Jandus, T. Lövgren, I. Luescher, S. Leyvraz, and V. Voelter for essential collaboration and advice. We are also thankful for the excellent help of C. Beauverd, P. Corthesy, C. Geldhof, L. Leyvraz, N. Montandon, and M. van Overloop.

This study was sponsored and supported by a grant from the Wilhelm Sander Foundation, the Swiss National Center of Competence in Research (NCCR) Molecular Oncology, the Ludwig Institute for Cancer Research, NY USA, the Swiss National Science Foundation grant 3200B0-118123, and the Oncosuisse grant OCS-01995-02-2007.

Original title: Similar functional competence of dominant and non-dominant CD8 T cell clonotypes revealed by single cell analysis

List of co-authors: Speiser DE, Wieckowski S, Gupta B, Iancu EM, Baumgaertner P, Romero P, Michielin O, and Rufer N

INTRODUCTION

Protective T-cell responses are characterized by strong initial clonal T-cell bursts arising from a relatively small number of highly specific naïve precursor T-cells [1]. Analysis of T-cell receptor (TCR) repertoires of protective virus-specific CD8 T-cells revealed that up to high frequencies of epitope-specific T-cells are composed of small numbers (≈5 to 50) of co-dominant clonotypes [2], yet having the ability to recognize the same pMHC complex. Along with the extraordinary high TCR selectivity, T-cells undergo profound cell activation and proliferation, resulting in frequency increase and memory/effector cell differentiation, assuring respectively T-cell survival, homing and long-term persistence, and strong effector function [3]. Among the currently identified correlates of protection, high frequency of naïve precursor T-cells, high antigen sensitivity (also defined as functional avidity), cross-reactivity to antigenic variants, and poly-functionality (including proficient cytotoxic activity and multiple cytokine production) appear essential to achieve best *in vivo* CD8 T-cell efficacy [4-11].

Naturally acquired self-antigen (tumor)-specific T-cell responses can be detected in most advanced cancer patients. However, they often fail to control or eliminate the disease, in contrast to many virus-specific CD8 T-cell responses (reviewed in [12, 13]). This likely reflects the impact of both central and peripheral tolerance in shaping self antigen-specific T-cell repertoires. Therapeutic vaccination against cancer aim of generating and/or boosting effective type 1 immune responses (Th1 and CD8 T-cell activation) to destroy tumor cells and prevent tumor progression. These goals are similar as for vaccines against viral diseases. There is a great need to characterize and determine the biological similarities and differences between protective (i.e. EBV- and CMV-specific) and non-protective (i.e. tumor-specific) T-cells.

Only limited data is available regarding T-cell clonotypes. Yet, clonotypic analyses provide great insight, mostly because T-cell clonotypes can be followed in a straightforward manner at any time and body location using the TCR as a clonotypic marker [14, 15]. For example, combined *ex vivo* analysis of T-cell differentiation and clonality allowed the identification of a naturally primed T-cell clone in a melanoma patient [14]. The progeny of this clone dominated the CD8 T-cell response to the tumor antigen Melan-A/MART-1 [14], similarly to the clonal expansions observed in virus-specific T-cell responses [7, 16, 17]. However, in these patients and healthy individuals, one can also find large numbers of low/(non)-dominant T-cell clonotypes among tumor-specific [15] and virus-specific [16] CD8 T-cells. Remarkably, not only the dominant, but also the subdominant virus-specific clonotypes are maintained stably over

years, keeping the TCR repertoire composition constant [16]. These observations raise the questions whether dominant T-cell clonotypes are sufficient, or whether low/(non)-dominant clonotypes are also functionally competent and required for protection.

Historically, research has mostly focused on dominant T-cell clonotypes, whereas the *in vivo* functions of non-dominant clonotypes remain poorly characterized, likely because of technical limitations. Therefore, we developed novel methods suitable for the *ex vivo* functional assessment of individual T-cells, combined with clonotypic characterization. With this strategy, we analyzed tumor-specific T-cells from melanoma patients, in parallel to protective EBV- and CMV-specific T-cells. The melanoma patients had received potent low dose synthetic vaccines composed of Melan-$A^{MART\text{-}1}{}_{26\text{-}35}$ peptide, CpG and Incomplete Freund's Adjuvant (IFA) that consistently induced strong and thus *ex vivo* detectable T-cell responses [18], even when using the weakly antigenic native tumor peptide [19].

Here, we report the preferential selection and expansion of several tumor-specific co-dominant clonotypes of intermediate to high frequencies, irrespective of whether native or analog peptide was used for vaccination. Similar to EBV-specific T-cell responses [16], these clonotypes made up the majority of the differentiated "effector" T-cells, but only 25% of the less-differentiated "effector-memory" cells. The latter is mostly composed of non-dominant clonotypes, thus demonstrating clonotype-dependent differentiation. Surprisingly, however, the acquisition of effector function was clonotype independent, as we found similar functional profiles in dominant and low/non-dominant T-cell clonotypes. Finally, effector functions were more pronounced after native than analog peptide vaccination. In summary, this study reveals that effector functions are determined primarily by antigen and the stage of T-cell differentiation, but are similar in all clonotypes participating in a CD8 T-cell response.

RESULTS

Strong expansion and effector cell differentiation of tumor-reactive CD8 T-cells following peptide vaccination. Fifteen HLA-A2^{pos} patients with advanced metastatic melanoma received monthly vaccinations consisting of either the native Melan-A^{MART-1} 26-35 unmodified peptide (EAAGIGILTV, i.e. "EAA") or the analog Melan-A^{MART-1} A27L modified heteroclitic peptide (ELAGIGILTV, i.e. "ELA"), combined with CpG 7909 and emulsified in IFA (Fig. 1A). Using fluorescent HLA-A2/peptide multimers for *ex vivo* analysis, high frequencies of Melan-A^{MART-1} specific CD8 T lymphocytes were detected in all patients, and highly increased as compared to before vaccination (defined as time 0; SI Fig. 1 and [20]). Tumor-reactive T-cells exhibited an effector-memory (EM; CD45RA^{neg}CCR7^{neg}, [21]) phenotype and included two distinct functional subsets based on CD28 expression [14, 15, 22, 23]; (i) CD28-positive (defined thereafter as EM28^{pos} or early differentiated) cells and (ii) CD28-negative (EM28^{neg} or effector-like) cells. Apart from a few exceptions (patients LAU 321, LAU 672 and LAU 936), we found progressive accumulation of differentiated effector EM28^{neg} Melan-A-specific T-cells, which appeared early in some patients and later in others, independent of whether patients received native or analog peptide (SI Fig. 1). The established T-cells were maintained over extended periods of time while patients continuously received monthly booster vaccinations.

Vaccination-induced T-cell responses are characterized by robust selection and expansion of particular clonotypes. We characterized in depth the ex vivo TCR repertoire diversity and clonal selection of tumor-reactive T-cells in patients vaccinated either with the native (EAA; n = 5) or the analog (ELA; n = 10) Melan-A peptide, as described previously [14]. Primed EM28^{pos} cells displayed large polyclonal TCR repertoires with a diverse usage of the 22 different BV families studied, and high variability in CDR3 size (SI Fig. 2A). However, 12 of the 15 patients showed progressive restrictions in TCR BV/CDR3 diversity from EM28^{pos} to EM28^{neg} T-cell subsets (Fig. 1B), which was accompanied with a strong increase in frequencies of co-dominant T-cell clonotypes found among the latter, more differentiated effector-like subset (Fig. 1C; SI Table 2 and SI Fig. 2B), irrespective of native or analog peptide used for vaccination. A striking observation was that the T-cell responses were dominated by individual clonotypes in several patients (e.g. LAU 618, BV17-1 and BV3-1; LAU 672, BV7-1; LAU 972, BV5-1; LAU 1013, BV13-1), in line with our previous report [14]. Despite that the proportion of non-dominant TCR sequences (termed as BV "other") was

much greater in EM28^{pos} than in EM28^{neg} T-cells, oligoclonal expansions of particular T-cell clonotypes were also found in the former subset, representing an average of 25% of the repertoire (SI Fig. 2C). Many of the dominant clonotypes identified in the differentiated EM28^{neg} subset were also found, though at much lower frequencies, in the EM28^{pos} compartment. Interestingly, in native peptide vaccinated patients, common T-cell clonotypes were more frequently distributed between both subsets. Altogether, these findings show that both clonotype selection and composition of vaccination-induced tumor-reactive T-cell responses along cell differentiation resembled closely to those observed for protective EBV-specific responses [16] (SI Fig. 2C). Yet, the proportion of non-dominant clonotypes was greater in vaccination-induced tumor-specific T cells compared to anti-viral responses.

Vaccination with native peptide rapidly induced clonotypes shared between early- and late-differentiated T-cell subsets. We next investigated the time course of establishment of dominant T-cell clonotypes following vaccination and their persistence over time (Fig. 2). To directly assess the presence of particular clonotypes *ex vivo* and their relative frequencies within distinct T-cell subsets, we used a modified RT-PCR protocol, enabling the detection of specific cDNAs after global amplification of expressed mRNAs from as few as five sorted T-cells [14, 24]. The unique TCR signature of each clonotype was subsequently determined by CDR3 size lengths, clonotype specific primers and/or sequencing of amplified products containing the CDR3 region [14]. In patients receiving the native peptide (EAA), transcript analysis revealed the emergence of dominant clonotypes of intermediate and high frequencies as early as 1 to 3 months after the start of vaccination (Fig. 2B and 2C), and this rapid selection was already evident within the early-differentiated EM28^{pos} subset (Fig. 2B; SI Fig. 3A). These findings contrasted with the clonotype kinetics observed in patients vaccinated with the analog peptide (ELA), where the T-cell repertoire was largely composed of single non-dominant clonotypes. In those patients, most of the dominant T-cell clonotypes appeared after 3 months, and thus reached similar frequencies as patients vaccinated with native peptide only at later time-points (Fig. 2A and 2C; SI Fig. 3A). We also observed that the number of dominant clonotypes shared between EM28^{pos} and EM28^{neg} subsets at early time-points ($\leq$ 3 months) after vaccination was greatly increased in the native compared to the analog cohort (SI Fig. 3B). In line with our previous reports [14, 15], repetitive vaccinations induced in both cohorts sustained tumor-specific T-cell responses and the persistence of co-dominant clonotypes over several months to years (Fig. 1A). Our data reveal the establishment

following therapeutic vaccination of relative few (between 7 to 15) co-dominant tumor-specific T-cell clonotypes and specific for each patient. We conclude that dominant clonotypes from the native peptide vaccination-induced responses appeared earlier and were more frequently shared between early- and late-differentiated T-cell subsets.

Enhanced expression of multiple effector mediators by native peptide vaccination-induced T-cells, closely resembling highly differentiated CMV-specific T-cells. To qualitatively assess the effect of native versus analog peptide vaccination, we developed techniques for combined *ex vivo* analysis of molecular and functional properties at the single-cell level (Fig. 3A and 3B; SI Fig. 4A). We found that most early-differentiated $EM28^{pos}$ T-cells issued from patients vaccinated with the analog/ELA peptide contained low detectable levels of mRNA coding for effector mediators such as IFN-γ, perforin, granzyme B and C-type killer cell lectin-like receptor CD94, while expressing measurable levels of mRNA coding for the costimulatory molecule CD27 and the cytokine receptor IL-7Rα (CD127). Increased expression of effector mediators and concomitant down-regulation of costimulatory and cytokine receptors was observed within ELA-specific $EM28^{neg}$ differentiated T-cells, similarly to the single-cell gene expression profiling depicted by CMV-specific T-cells upon cell differentiation. EBV-specific T-cells also presented distinct mRNA expression patterns along cellular differentiation, but globally these cells remained less differentiated than tumor- or CMV-specific T-cells, in agreement with our recent report [16]. A remarkable finding was that the tumor-reactive T-cells generated following native peptide vaccination exhibited similar detectable levels of effector mediators than those observed in CMV-specific T-cells. Importantly, such expression patterns were already found within the $EM28^{pos}$ compartment, despite the co-expression of early-differentiated CD27 and IL-7Rα gene transcripts (Fig. 3A and 3B). These cells also showed more poly-functional expression profiles compared with the corresponding $EM28^{pos}$ T-cells specific for ELA and EBV epitopes (SI Fig. 4B). mRNA content correlated with protein expression, as confirmed by extended *ex vivo* multi-parameter flow cytometry analyses of T-cells from all 15 vaccinated melanoma patients as well as 5 healthy individuals with persistent herpes virus infections (Fig. 4; SI Fig. 5). Thus, native peptide vaccination, in contrast to analog peptide, readily induced expression of a comprehensive set of functionally key molecules in the early-differentiated $EM28^{pos}$ T-cell subset.

A hierarchical clustering performed on a total of 529 single-cell samples identified 5 distinct clusters based on the differential co-expression patterns of the 6 studied genes (Fig. 3C). The Heat-map analysis further allowed determining the repartition of these clusters within the single-cell samples of each T-cell subset, showing that antigen-specific T-cells could be divided into two major groups/families. The first one was composed of the early-differentiated $EM28^{pos}$ T-cells specific for the ELA, EBV and CMV epitopes, and included the EMRA EBV-specific subset. The second group was formed by the differentiated effector-like $EM28^{neg}$/EMRA ELA-, EAA-, and CMV-specific T-cells, and strikingly also comprised the early-differentiated $EM28^{pos}$ T-cells induced by the native/EAA peptide. Altogether, our results indicate that vaccination with the native but not analog tumor antigen generated CD8 T-cell responses of enhanced cell activation and poly-functionality *in vivo*, independently of CD28, CD27 and IL-7Rα co-expression, and resembling highly differentiated CMV-specific responses.

Both T-cell differentiation and the peptide used for vaccination determine the functional profile of individual T-cell clonotypes. The powerful single-cell based approach allowed for the first time to analyze *in vivo* gene expression of (multiple representatives of) individual T-cell clonotypes. By this strategy, we compared clonotype performance after vaccination with analog versus native peptide based on their frequencies. Profiles of dominant T-cell clonotypes (Fig. 5A) largely overlapped those observed for the tumor-specific subsets from which they were respectively isolated (SI Fig. 4B). For instance, the dominant BV3-1 clonotype from patient LAU 618/ELA shared the gene expression profile of early-differentiated $EM28^{pos}$ subsets from analog peptide vaccinated patients. Conversely, the profiles of the dominant native peptide vaccination-induced BV13-1 clonotype from patient LAU 1013 were highly poly-functional, thus corresponding to the overall gene expression profiles found within the respective $EM28^{pos}$ and $EM28^{neg}$ subset. Strikingly, gene expression signatures of non-dominant tumor-reactive T-cells (Fig. 5B) correlated also tightly with the subset of origin (e.g. $EM28^{pos}$ or $EM28^{neg}$) and the type of peptide used for vaccination (e.g. native or analog peptide). Similar observations were made for the dominant and low/(non)-dominant clonotypes found in EBV- and CMV-specific immune responses. In summary, we found that the functional profile of dominant and low/non-dominant T-cell clonotypes was primarily determined by the antigen and the stage of differentiation.

Efficient target cell killing by T-cells of both dominant and non-dominant clonotypes from patients vaccinated with native peptide. We assessed the ability of native and analog peptide vaccination-induced tumor-specific T-cells to recognize and kill Melan-A-expressing tumor cells (Fig. 6A and 6B, SI Fig. 6A). As expected, most T-cell clones derived from the differentiated effector-like $EM28^{neg}$ subset were able to kill the Melan-A-expressing tumor cell line Me 290, irrespectively of the peptide used for vaccination. However, T-cell clones derived from the early-differentiated $EM28^{pos}$ subset following analog peptide vaccination were often deficient in cytotoxic function. In contrast, a large majority of T-cell clones derived from the same $EM28^{pos}$ subset from patients vaccinated with the native peptide efficiently killed the Me 290 cell line. Strikingly, this occurred regardless of whether these clones were of high (dominant clonotypes) or very low (non-dominant clonotypes) frequencies (Fig. 6B). Conclusions with respect to the *in vivo* status of T-cells are possible because these functional results correspond to gene and protein expression data (Fig. 3 and Fig. 4). Furthermore, we have previously demonstrated that our T-cell clones maintained their *in vivo* programmed phenotypic and functional properties despite several weeks of *in vitro* culture [25].

The functional avidity for the pMHC of these clones was determined by cytotoxic assays against $HLA\text{-}A2^{pos}$ T2 cells in the presence of graded peptide concentrations (Fig. 6C and SI Fig. 6B). Native peptide vaccination-induced T-cells derived from $EM28^{pos}$ cells were again significantly superior in regards to maximal lysis capacity, compared to the killing responses obtained from the corresponding subset upon analog peptide vaccination. As observed for tumor cell killing assays, maximal T2 lysis was found for both dominant and non-dominant clonotypes issued from native peptide vaccination. Regarding functional avidity (EC_{50}), all native and analog peptide-derived $EM28^{pos}$ T-cell clones behaved similarly, with 50% maximal lysis of T2 cells found at comparable peptide doses (and no statistically differences). Yet, the latter subset showed a high degree of heterogeneity where a substantial fraction of the T-cell clones depicted poor to no killing ($EC_{50} > 10^{-6}$ M), contrasting with the native peptide vaccination-induced clones displaying more homogeneous killing.

Collectively, these data revealed differential cytotoxicity of analog peptide generated T-cell clones depending on the *in vivo* differentiation stage, and consistent with our previous report [25]. In contrast to analog peptide vaccination, strong cytolytic activity and potent functional avidity, regardless of the type of subset (i.e. clones isolated from $EM28^{pos}$ or $EM28^{neg}$) was observed after vaccination with the native peptide. This finding may likely be attributed to the

stronger expression of multiple effector molecules found within $EM28^{pos}$ T-cells from native versus analog peptide vaccination (Fig. 3 and 4). Importantly, similar efficient target cell killing (maximal lysis and EC_{50}) was observed in all dominant and non-dominant T-cell clonotypes, further supporting the notion that vaccination with native peptide was very successful at inducing robust cytolytic activation of most T-cells.

DISCUSSION

Peptide-based cancer vaccines are often performed with altered "analog" peptide antigens that have been optimized for enhanced MHC class I binding, resulting in superior T-cell immunogenicity [26]. This is illustrated in studies where the immunodominant HLA-A*0201-restricted peptide of the melanoma antigen Melan-A$^{MART\text{-}1}_{26\text{-}35}$ (EAAGIGILTV) was modified by an Ala to Leu substitution at position 27 (A27L; ELAGIGILTV) [18, 27-29]. This model provides ideal opportunities to assess possible effects of a small antigenic difference on the *in vivo* quality (e.g. effector functions, stage of differentiation, and clonotype selection) of the generated T-cell responses. Compared with vaccination with the analog Melan-A peptide, we previously reported that native peptide induced T-cells with increased activation and effector function [19]. These observed differences could not be explained by structurally distinct TCRs, since vaccination with native and analog peptide triggered largely overlapping TCR repertoires with structurally conserved features of TCR$\alpha\beta$ chains [30]. Here, we demonstrate that the superior tumor activity by native peptide induced T-cells is because effector functions developed properly in nearly all dominant and low/non dominant tumor-specific T-cell clonotypes. In contrast, many T-cells remained poorly functional after vaccination with analog peptide, despite sharing similar clonotype-dependent differentiation. Thus, a single amino acid substitution within a peptide vaccine can have significant consequences on the quality of the T-cell response.

The present study allowed for the first time to determine effector function-associated gene expression by individual T-cells *ex vivo*, including low/non-dominant clonotypes (Fig. 7). Indeed, single-cell analysis provides reliable quantification of individual cells expressing a particular gene, as confirmed by protein expression analyses. Moreover, our strategy is highly sensitive to identify tumor-reactive T-cell clonotypes and to assess their frequencies (Fig. 7), and is in excellent agreement with the data obtained by the *in vitro* T-cell cloning approach (Fig. 1; [16]) (Gupta, Iancu et al., *manuscript in preparation*). An analogous approach has been previously and successfully applied to study cell heterogeneity during *in vivo* CD8 differentiation [23, 31]. Here we found that anti-tumor T-cell effector function is primarily determined by the type of peptide used for vaccination (native versus analog) and is not inherent of a given T-cell clonotype or of its prevalence (dominant versus non-dominant). Moreover, similar distributions in effector gene expression signatures were found between T-cell clonotypes issued from the same subset of differentiation (Fig. 7). Comparable observations were made for EBV- and CMV-specific T-cells, indicating that the functional

profile of individual T-cells is also influenced by the differentiation status. As a consequence, most if not all clonotypes from a given subset of differentiation and participating in a tumor (self) or viral (non-self) T-cell response may be equally competent. Selection of a T-cell repertoire composed of low/(non)-dominant and dominant clonotypes could serve to promote clonotypic diversity, while maintaining functional competence. These results are consistent with the report by Messaoudi and colleagues [32] that a diverse TCR repertoire but not a restricted one can mobilize protective antigen-specific T-cells of high avidity and efficient target cell killing.

Our data also show that a synthetic vaccine (i.e. decapeptide, CpG and IFA [18]) was able to trigger a similar composition of T-cell clonotypes as in viral infections, [7, 17], and particularly in EBV-specific T-cell responses [16]. Responding T-cells were composed of clonotypes of varying frequencies (dominant, subdominant and non-dominant), yet the proportion of each frequency-based clonotypes was dependent on the differentiation stage (Fig. 7). Late-differentiated $EM28^{neg}$ ("effector-like") consisted primarily of patient specific dominant (high frequency) and subdominant (low frequency) clonotypes with long-term persistence. In contrast, the early-differentiated $EM28^{pos}$ subset (that includes effector-memory cells) contained mostly non-dominant clonotypes with only a small fraction (25%) of co-dominant T-cell clonotypes. Thus, clonotypic diversity was mostly found within the effector-memory subset, contrasting with advanced differentiation stages that contained some clonotypes that were enriched, while others were not. This process is likely to be clonotype-dependent, consistent with studies on T-cells specific for persistent viruses [7, 17], and highlighting the importance of the structural composition of the TCR repertoire for T-cell differentiation. Moreover, many tumor-specific clonotypes identified in the late-differentiated effector-like subset were also found within the pool of less-differentiated "effector-memory" cells, albeit at much lower frequencies. Co-existence of identical clonotypes as both effector-memory and effector T-cells has also been described for human T-cells specific for influenza matrix protein peptide [33] and HIV epitopes [17]. Together, these observations are in line with recent findings by Gerlach and coworkers [34], showing that individual naive T-cells have multiple fates and can differentiate into both memory and effector T-cell subsets.

What are the processes involved during recruitment and subsequent maintenance of dominant and low/(non)-dominant clonotypes along a T-cell response? The strength of the TCR-ligand interactions, also defined as TCR binding affinity/avidity, has been proposed to represent one of the driving forces underlying clonal selection and expansion. Consistent with this notion,

very weak interactions were sufficient for T-cell activation and induction of functional memory cells, while stronger TCR ligation allowed the preferential expansion of T-cells with increased affinity/avidity [35]. Price and colleagues have shown that dominant T-cell clonotypes specific for persistent herpes viruses exhibited increased pMHC binding avidity, compared to subdominant clonotypes, mostly characterized by a greater dependency on the MHCI-CD8 interactions [7]. These findings provide evidence that the binding avidity for the antigen shapes clonal dominance, while the CD8 co-receptor may compensate for those differences in TCR affinity/avidity by keeping a diverse and heterogeneous T-cell clonotype repertoire within a physiological range of functional competence [36]. Whether similar physical parameters may also apply for vaccination-induced tumor-specific T-cell responses remains unclear. Future investigations should include binding analysis to pMHC, as well as assessing expression levels of accessory and/or costimulatory molecules by low/(non)-dominant and dominant clonotypes.

A remarkably finding was that vaccination with native but not analog peptide was more rapid and more efficient at inducing the expression of multiple effector molecules in nearly all Melan-A-specific T-cell clonotypes. This correlated with efficient target cell killing. Consequently, both native-peptide vaccination-induced T-cell subsets ($EM28^{pos}$ and $EM28^{neg}$), closely resembled each other, and to the highly differentiated CMV-specific T-cells (Fig. 7). These data refine our current view of the process of T-cell differentiation, as they indicate that progressive up-regulation of cytolytic activity does not necessarily require the stepwise loss of costimulatory (CD27, CD28) and cytokine receptor (IL-7Rα) expression. Previous reports have described a hierarchical order of T-cell differentiation stages, from naïve to CM, $EM28^{pos}$, $EM28^{neg}$ and EMRA cells [21-23, 37, 38]. Specifically, Monteiro and colleagues showed that cellular differentiation (loss of CCR7/CD27/CD28 co-expression) led to a progressive up-regulation of multiple "killer" mediators by the same cell [23]. This report together with our own observations [22] has provided a tight correlation between particular cell surface markers (e.g. $CCR7^{+/-}$, $CD28^{+/-}$, and $CD27^{+/-}$) and T-cell functional properties. While these studies were performed on circulating "bulk" CD8 T-cells, an alternative picture became apparent when assessing virus antigen-specific T-cells. Indeed, despite showing distinct expression patterns along with cell differentiation, CMV-specific cells also expressed globally higher levels of CD94, CD57, IFN-γ, perforin and granzyme B than EBV-specific cells (Fig. 7; [16]). In line with this observation, we show here that vaccination with the native self/tumor Melan-A peptide was able to further enhance the expression of effector mediators among

tumor-specific T-cells despite their co-expression of early-differentiated surface markers, CD27, CD28 and IL-7Rα.

What are the mechanisms causing accelerated differentiation and enhanced expression of effector mediators observed following vaccination with the native peptide? Possibly, vaccination with native peptide may recruit T-cells of superior TCR affinity/avidity, selected to overcome the lower peptide binding to MHC (the analog peptide binds 10 times more stably to HLA-A2 than the native peptide [27]). Alternatively, high avidity T-cells generated by analog peptide vaccination may be more susceptible to apoptosis. Furthermore, T-cell priming and activation may depend on the relative signals during interaction with APCs, involving costimulation and cytokines. The differences observed in effector functions between native or analog peptide vaccination-induced T-cells may also be independent of the primary TCR structure, and rather involve differential TCR and coreceptor supramolecular organization [39, 40] as well as basal T-cell activation (e.g. phosphorylation) status [41].

Our current study shows that clonotype-dependent and clonotype-independent processes, respectively, shape the structural and functional composition of tumor-specific vaccination-induced T-cells, similarly to EBV- and CMV-specific T-cell responses. High-resolution characterization of individual T-cells at the clonotype level as shown here, provide the basis to identify the biological benchmarks associated with protective T-cell immunity, contributing to the rationale development of vaccines.

FIGURE LEGENDS

Figure 1. TCR BV repertoire diversity analysis and quantification of Melan-A-specific T-cell clonotypes. *A*, Fifteen patients vaccinated with the analog (ELA; n = 10) or the native (EAA; n = 5) peptide were followed over time (# of monthly vaccinations, duration of vaccination, see *Supporting Information*) and characterized for their specific T-cell immune responses (e.g. persistence of T-cell clonotypes over time). Mo, months. *B*, cDNA pools (50 cells) generated from *ex vivo* $EM28^{pos}$ and $EM28^{neg}$ tumor-specific T-cells sorted from peripheral blood from patients vaccinated with the native or analog peptide were amplified by PCR using 22 BV-specific primers, and subjected to electrophoresis (TCR BV spectratyping). BV repertoire diversity is expressed as the total number of amplified BV-CDR3-BC products of different lengths within each positive BV families. The analysis comprised blood samples collected at 1 to 3 separated time-points per patient following vaccination. * $0.01 < P < 0.05$, *** $P < 0.005$ (two-tailed unpaired *t* test). *C*, Frequencies of Melan-A-specific T-cell clonotypes determined by CDR3 size lengths, sequencing and clonotypic PCR. This part of the study was performed on *in vitro* generated T-cell clones from patients vaccinated either with analog peptide (LAU 618, n = 513; LAU 672, n = 161) or native peptide (LAU 972, n = 139; LAU 1013, n = 134). Time-points after vaccination were 14 mo (LAU 618), 16 mo (LAU 672), 8 mo (LAU 972) and 8 mo (LAU 1013), respectively. Each clonotype (frequency ≥ 1%) is indicated and each TCR BV family is color-coded. Non-dominant clonotypes are designed as "BV other" and are comprised of clonotypes of unique TCR BV/CDR3 sizes and/or BV-CDR3-BC sequences as determined by capillary electrophoresis and sequencing.

Figure 2. Comparison of early and late time-points of TCR BV repertoire diversity and clonotype frequency of circulating Melan-A-specific CD8 T-cell subsets analyzed *ex vivo*. *A* and *B,* BV spectratyping was performed on cDNA obtained from individually sorted 5-cell samples (n = 8 to 20) of specific $EM28^{pos}$ (*upper panel*) and $EM28^{neg}$ (*lower panel*) T-cells isolated from patients at the indicated time-points after vaccination with the analog peptide (*A*) or the native peptide (*B*). Dominant TCR clonotypes (defined as identical BV-CDR3-BC sequence found at least twice) and non-dominant single TCR clonotypes (defined by their unique TCR BV/CDR3 size length and/or BV-CDR3-BC sequence). Data are represented as the total number (y-axis) of dominant (filled area) and single (grey area) clonotypes of defined TCR BV family (x-axis) versus defined CDR3 size length (z-axis). Representative examples are depicted. *C*, Complete set of data (9 and 5 patients vaccinated with the analog or

native peptide, respectively) representing the proportion of single *(left panel*) and dominant (*right panel*) clonotypes identified within the EM28^{neg} subset of the indicated patient cohort and time-point after vaccination. Of note, patient LAU 444 (vaccinated with analog peptide) was not included in this analysis, since we identified a single dominant T-cell clonotype of high frequency prevailing already before immunotherapy, which was apparently naturally primed and rapidly and predominantly boosted upon vaccination [14]. Early time-point, 1 to 3 months; late time-point, > 3 to 21 months. Dominant clonotypes were classified according to their relative frequencies among tumor-specific EM28^{neg} subsets as > 25%, high frequency (empty symbols) and 1-25%, intermediate frequency (filled symbols). Due to the limited amount of sorted EM28^{neg} T-cells from patients vaccinated with the analog peptide at early time-points compared to late time-points, reduced numbers of samples were analyzed. *P*-values were calculated with two-tailed unpaired *t* test.

Figure 3. Gene expression profiling of single T-cells sorted *ex vivo* upon gating on tumor- and virus-specific CD8 T-cell subsets. *A*, Single-cells were isolated from EM28^{pos} and EM28^{neg} (patients vaccinated either with analog/ELA or native/EAA peptide), and from EM28^{pos} and EMRA (EBV- and CMV-specific T-cells from the healthy individual BCL8) T-cell subsets, subjected to global cDNA amplification, and analyzed by specific PCR amplification of *CCR7, CD27*, *IL-7Rα*, *CD94*, *IFN-γ*, *perforin* and *granzyme B* known to be differentially expressed at distinct stages of cell differentiation [14, 22]. *GAPDH* gene expression was analyzed as quality control. Positive PCRs are depicted in red and negative ones in blue. Compiled data are shown per subset and per patient/healthy individual, where each line represents a single T-cell. Analysis was performed at the same time-points after vaccination as those depicted in Fig. 1C. *B*, Complete sets of data of the proportion of each expressed gene in early- (EM28^{pos}) or late- (EM28^{neg}, EMRA) differentiated subsets from patients vaccinated with analog peptide (LAU 618, ●; LAU 672, ■) and native peptide (LAU 1013, ○; LAU 972, □), and from healthy donors BCL8 (EBV, △; CMV, ◇) and BCL6 (CMV, ▽). *C*, A hierarchical clustering (*left panel*) of the complete data sets (n = 529 single-cell samples) depicted in (*A*), based on Euclidean distance between samples with the UPGMA clustering method. The cluster dendrogram identifies 5 distinct clusters (minimum similarity set to 0.375). The repartition of these clusters within the single-cell samples of each EM28^{pos} and EM28^{neg} T-cell subset (specific for ELA, EAA, EBV or CMV) was then determined by Heat-map analysis (*right panel*). Of note, single cell samples from EM28^{pos} antigen-specific subsets

were mostly found within clusters I-III (IFN-γ^{low}, $perf^{low}$ and $granB^{low}$), whereas those from $EM28^{neg}$ subsets were classified in clusters II, IV and V (IFN-γ^{high}, $perf^{high}$ and $granB^{high}$).

Figure 4. *Ex vivo* expression of effector mediators within tumor- and virus-specific CD8 T-cell subsets. *A*, The proportion of CD57, perforin and granzyme B protein expression among antigen-specific $EM28^{pos}$ and $EM28^{neg}$ subsets was determined by multi-parameter flow cytometry. The dotted line was set according to the gating obtained on bulk $CD8^{pos}$ naive T-cells known to be $CD57^{neg}perforin^{neg}granzymeB^{neg}$. Representative examples are shown. *B*, A complete set of data was obtained from melanoma patients following analog (ELA, n = 10) or native (EAA, n= 5) peptide vaccination, and from healthy individuals with EBV (n= 5) and/or CMV (n = 5) specific T-cell responses. * $0.01 < P < 0.05$, ** $0.005 < P < 0.01$, *** $P < 0.005$ (two-tailed unpaired *t* test).

Figure 5. Characterization of gene expression profiles combined with clonotyping. Poly-functional gene expression was determined for representative dominant (*A*) and non-dominant (*B*) tumor- and virus-specific T-cell clonotypes, upon *ex vivo* single-cell sorting (n = 529) of $EM28^{pos}$ and $EM28^{neg}$/EMRA T-cells. Dominant clonotypes (*A*) are defined according to their relative frequencies within a specific subset as high (> 10 %) or intermediate (1-9 %) frequency, and non-dominant TCRs (*B*) as frequencies < 1%. The pie charts illustrate the co-expression profiles of *CD94*, *IFN-γ*, *perforin* and *granzyme B* within the single-cell samples.

Figure 6. Tumor cell killing and efficiency of antigen recognition. Tumor-specific T-cell clones were generated *in vitro* by limiting-dilution from blood samples corresponding to the same time-points after vaccination as those depicted in Fig. 2. *A*, Tumor reactivity for the melanoma cell lines Me 290 ($A2^+$/Melan-A^+) and NA8 ($A2^+$/Melan-A^-) in absence or presence of Melan-A analog peptide (1 μM), at an effector:target ratio of 30:1. Each line represents the result of an individual clone derived from $EM28^{pos}$ or $EM28^{neg}$ subsets from patients vaccinated either with analog (ELA; n = 153) or native peptide (EAA; n = 80). T-cells were grouped for low, intermediated, and high target cell lysis (i.e. < 20% (red), 20-60% (yellow), and >60% (green)). *B*, Complete data representing specific lysis of the Melan-A^+ Me 290 tumor cell line in the absence of exogenous Melan-A peptide (10:1; effector:target ratio) by dominant and non-dominant T-cell clones derived from $EM28^{pos}$ and $EM28^{neg}$

subsets of patients vaccinated with analog (grey whiskers) or native peptide (empty whiskers). *C*, The relative TCR avidity was compared using T2 target cells ($A2^{+}/TAP^{-/-}$) pulsed with graded concentrations of analog/ELA Melan-A_{26-35} peptide. $EM28^{pos}$ and $EM28^{neg}$ T-cells were defined as dominant and non-dominant BV clonotypes. Complete data representing maximal lysis (*upper panel*) and EC_{50} (e.g. peptide concentration required to achieve 50% of maximal lysis; *lower panel*). We used the same clones as in *A* and *B*. Clones with undetectable lytic activity ($EC_{50} > 10^{-6}$ M and/or maximal lysis < 20%) are symbolized as single dots above the y-axis and were not included in the statistical evaluations. * $0.01 < P < 0.001$, ** $0.001 < P < 0.0001$, *** $P < 0.0001$ (two-tailed unpaired *t* test).

Figure 7. Clonotypic and functional composition of vaccination-induced tumor-specific and virus-specific T-cell repertoire revealed by *ex vivo* single cell analysis. Each clonotype is represented by its frequency (*inner circle*) and its poly-functional effector gene expression profile (*outer circle*). Increased frequency and poly-functional gene expression (co-expression of *CD94*, *IFN-γ*, *perforin* and *granzyme B*) are depicted as progressive color gradients. Data from four patients vaccinated with the analog (LAU 618 and LAU 672) and native (LAU 1013 and LAU 972) Melan-A peptide, and from two healthy individuals (BCL6 and BCL8; EBV and CMV-specific T-cell responses) are shown.

METHODS

Patients and vaccination, and healthy blood donors

Fifteen HLA-A*0201-positive patients with stage III/IV metastatic melanoma were included in a phase I prospective trial of the Ludwig Institute for Cancer Research and the Multidisciplinary Oncology Center, approved by institutional review boards and regulatory agencies [18, 19]. Patients received monthly low-dose vaccinations injected subcutaneously with 100 μg of either the Melan-$A^{MART\text{-}1}{}_{26\text{-}35}$ unmodified native peptide (EAAGIGILTV) or the Melan-$A^{MART\text{-}1}{}_{26\text{-}35}$ analog A27L peptide (ELAGIGILTV), mixed with 0.5 mg CPG 7909 / PF-3512676 (Pfizer and Coley Pharmaceutical Group) and emulsified in Incomplete Freund's Adjuvant (IFA) (Montanide ISA-51; Seppic)[18]. Leukapheresis from two healthy donors (BCL6 and BCL8) with positive EBV- and CMV-specific CD8 T-cell responses were collected upon informed consent as recently described [16].

Cell preparation and flow cytometry

Ficoll-Paque centrifuged peripheral blood mononuclear cells (PBMCs) were cryopreserved in RPMI 1640, 40% FCS and 10% DMSO. Synthesis of phycoerythrin (PE)-labeled HLA-A*0201/peptide multimers with A27L Melan-$A^{MART\text{-}1}{}_{26\text{-}35}$ (ELAGIGILTV), EBV $BMLF1_{280\text{-}288}$ (GLCTLVAML), and CMV $pp65_{495\text{-}503}$ (NLVPMVATV) was prepared as described previously [42]. Before staining, $CD8^{pos}$ T-cells were positively enriched using a MiniMACS device (Miltenyi Biotech, Bergish Gladbach, Germany) resulting in > 90% $CD3^{pos}CD8^{pos}$ cells. Cells were stained in PBS, 0.2% BSA, 50 μM EDTA with multimers (1 μg/ml, 60 min, 4°C) and then with appropriate mAbs (20 min, 4°C), and sorted into defined sub-populations on a FACSVantage SE or a FACSAria (BD PharMingen, San Diego, CA) or immediately analyzed on a LSR II^{TM} flow cytometer (BD Biosciences) as described in the Supplemental Information. For dead cell exclusion, cells were stained with Live/Dead Fixable Dead Cell violet stain (Molecular Probes / Invitrogen). Intracellular content of granzyme B and perforin was measured in freshly isolated $CD8^{pos}$ T lymphocytes without previous stimulation as described elsewhere [14]. Data were analyzed using CellQuest (BD Biosciences) or FlowJo (TreeStar) software.

Generation of T-cell clones

HLA-A2/$multimer^{pos}$ $CD8^{pos}$ T-cell subsets ($EM28^{pos}$, $EM28^{neg}$, and EMRA) were sorted by flow cytometry [14, 16], cloned by limiting dilution, and expanded in RPMI 1640 medium

supplemented with 8% human serum, 150 U/ml recombinant human IL-2 (rhIL-2; a gift from GlaxoSmithKline), 1 µg/ml phytohemagglutinin (PHA; Sodiag, Losone, Switzerland) and 1 × 10^6/ml irradiated allogeneic PBMC (3000 rad) as feeder cells. T-cell clones were expanded by periodic (every 15 days) restimulation with PHA, irradiated feeder cells, and rhIL-2.

cDNA preparation and amplification

cDNA preparation, cDNA amplification and PCR were performed as described in Supplemental Information and elsewhere [24]. In brief, single-cell or 5-cell aliquots were sorted with a FACSVantage SE or FACSAria machine into 96-V bottom plates containing lysis/reverse transcription mix for direct cDNA synthesis. cDNA from single-cell or 5-cell aliquots was precipitated, and global cDNA amplification by RT-PCR was performed following the addition of an homopolymer d(A) sequence to the 3'-OH end. 10^5 cells from T-cell clones were processed through direct lysis and cDNA synthesis without undergoing the global cDNA amplification procedure.

Gene expression and TCR BV clonotype repertoire analysis

Single-cell samples were subjected to specific PCR reactions using the primers to detect *GAPDH, CD3, CCR7, CD27, CD94, IFN-γ, perforin and granzyme B* mRNA transcripts that are described in the Supplemental Information. TCR BV CDR3 spectratyping, sequencing and clonotyping were performed as detailed in the Supplemental Information, and recently [30]. All *ex vivo* single-cell, 5-cell or *in vitro* T-cell clone cDNA samples, isolated from defined tumor-specific T-cell subsets ($EM28^{pos}$ or $EM28^{neg}$) from patients vaccinated either with native or analog peptide were processed with the same rigorous approach to allow direct comparison between individuals. TCR Vβ usage and sequences were described according to the Arden nomenclature [43]. Term of "dominant clonotype" refers to a nucleotide sequence found at least twice in a given patient and time-point (> 1% of frequency) [30].

Chromium release and tumor recognition assays

Lytic activity and antigen recognition was assessed functionally in 4-h ^{51}Cr-release assays using T2 target cells (HLA-A*0201$^+$/Melan-A$^-$) pulsed with serial dilutions of the native Melan-$A^{MART\text{-}1}{}_{26\text{-}35}$ peptide (EAAGIGILTV) or of the analog Melan-$A^{MART\text{-}1}{}_{26\text{-}35}$ A27L (ELAGIGILTV) [44]. The percentage of specific lysis was calculated as 100 × (experimental – spontaneous release)/(total – spontaneous release). Similarly, the specific antigen recognition

lytic activity of the Melan-A^{MART-1}-specific T-cell clonotypes was assessed against the melanoma cell lines NA8 (HLA-$A2^+$/Melan-A^-) and Me 290 (HLA-$A2^+$/Melan-A^+) in the presence or absence of the indicated peptide at the indicated concentration.

Statistical and hierarchical clustering analyses

The results were analyzed by unpaired two-sample *t* test and log sigmoid curve fitting using GraphPad Prism version 5.03 (GraphPad Software, San Diego, CA). Hierarchical agglomerative clustering and dendrogram display of gene expression data were performed with HCE (Hierarchical Clustering Explorer) version 3.5 (http://www.cs.umd.edu/hcil/hce/). All PCR results were encoded into a data matrix in which the assigned value was +1 for a positive PCR product and 0 for a negative PCR product. The data were examined without normalization/transformation using Euclidean distance with the Unweighted Pair Group Mean Arithmetic (UPGMA) clustering method. Control genes (*GAPDH* and *CCR7*) were not included during clustering analysis.

REFERENCES

1. Blattman, J.N. *et al.* Estimating the precursor frequency of naive antigen-specific CD8 T cells. *J Exp Med* 195, 657-664 (2002).
2. Nikolich-Zugich, J., Slifka, M.K. & Messaoudi, I. The many important facets of T-cell repertoire diversity. *Nat Rev Immunol* 4, 123-132 (2004).
3. Gourley, T.S., Wherry, E.J., Masopust, D. & Ahmed, R. Generation and maintenance of immunological memory. *Semin Immunol* 16, 323-333 (2004).
4. Speiser, D.E., Kyburz, D., Stubi, U., Hengartner, H. & Zinkernagel, R.M. Discrepancy between in vitro measurable and in vivo virus neutralizing cytotoxic T cell reactivities. Low T cell receptor specificity and avidity sufficient for in vitro proliferation or cytotoxicity to peptide-coated target cells but not for in vivo protection. *J Immunol* 149, 972-980 (1992).
5. Almeida, J.R. *et al.* Superior control of HIV-1 replication by CD8+ T cells is reflected by their avidity, polyfunctionality, and clonal turnover. *J Exp Med* 204, 2473-2485 (2007).
6. Lichterfeld, M. *et al.* Selective depletion of high-avidity human immunodeficiency virus type 1 (HIV-1)-specific CD8+ T cells after early HIV-1 infection. *J Virol* 81, 4199-4214 (2007).
7. Price, D.A. *et al.* Avidity for antigen shapes clonal dominance in CD8+ T cell populations specific for persistent DNA viruses. *J Exp Med* 202, 1349-1361 (2005).
8. Appay, V., Douek, D.C. & Price, D.A. CD8+ T cell efficacy in vaccination and disease. *Nat Med* 14, 623-628 (2008).
9. Seder, R.A., Darrah, P.A. & Roederer, M. T-cell quality in memory and protection: implications for vaccine design. *Nat Rev Immunol* 8, 247-258 (2008).
10. Almeida, J.R. *et al.* Antigen sensitivity is a major determinant of CD8+ T-cell polyfunctionality and HIV-suppressive activity. *Blood* 113, 6351-6360 (2009).
11. Price, D.A. *et al.* Public clonotype usage identifies protective Gag-specific CD8+ T cell responses in SIV infection. *J Exp Med* 206, 923-936 (2009).
12. Romero, P. *et al.* Antigenicity and immunogenicity of Melan-A/MART-1 derived peptides as targets for tumor reactive CTL in human melanoma. *Immunol Rev* 188, 81-96 (2002).
13. Boon, T., Coulie, P.G., Van den Eynde, B.J. & van der Bruggen, P. Human T cell responses against melanoma. *Annu Rev Immunol* 24, 175-208 (2006).
14. Speiser, D.E. *et al.* A novel approach to characterize clonality and differentiation of human melanoma-specific T cell responses: spontaneous priming and efficient boosting by vaccination. *J Immunol* 177, 1338-1348 (2006).
15. Derre, L. *et al.* In Vivo Persistence of Codominant Human CD8+ T Cell Clonotypes Is Not Limited by Replicative Senescence or Functional Alteration. *J Immunol* 179, 2368-2379 (2007).
16. Iancu, E.M. *et al.* Clonotype selection and composition of human CD8 T cells specific for persistent herpes viruses varies with differentiation but is stable over time. *J Immunol* 183, 319-331 (2009).
17. Meyer-Olson, D. *et al.* Clonal expansion and TCR-independent differentiation shape the HIV-specific CD8+ effector-memory T-cell repertoire in vivo. *Blood* 116, 396-405.
18. Speiser, D.E. *et al.* Rapid and strong human CD8+ T cell responses to vaccination with peptide, IFA, and CpG oligodeoxynucleotide 7909. *J Clin Invest* 115, 739-746 (2005).
19. Speiser, D.E. *et al.* Unmodified self antigen triggers human CD8 T cells with stronger tumor reactivity than altered antigen. *Proc Natl Acad Sci U S A* 105, 3849-3854 (2008).
20. Speiser, D.E. *et al.* In vivo activation of melanoma-specific CD8(+) T cells by endogenous tumor antigen and peptide vaccines. A comparison to virus-specific T cells. *Eur J Immunol* 32, 731-741 (2002).
21. Sallusto, F., Lenig, D., Forster, R., Lipp, M. & Lanzavecchia, A. Two subsets of memory T lymphocytes with distinct homing potentials and effector functions. *Nature* 401, 708-712 (1999).
22. Romero, P. *et al.* Four functionally distinct populations of human effector-memory CD8+ T lymphocytes. *J Immunol* 178, 4112-4119 (2007).

23. Monteiro, M., Evaristo, C., Legrand, A., Nicoletti, A. & Rocha, B. Cartography of gene expression in CD8 single cells: novel CCR7- subsets suggest differentiation independent of CD45RA expression. *Blood* 109, 2863-2870 (2007).
24. Rufer, N., Reichenbach, P. & Romero, P. Methods for the ex vivo characterization of human CD8+ T subsets based on gene expression and replicative history analysis. *Methods Mol Med* 109, 265-284 (2005).
25. Barbey, C. *et al.* IL-12 controls cytotoxicity of a novel subset of self-antigen-specific human CD28+ cytolytic T cells. *J Immunol* 178, 3566-3574 (2007).
26. Rosenberg, S.A., Yang, J.C. & Restifo, N.P. Cancer immunotherapy: moving beyond current vaccines. *Nat Med* 10, 909-915 (2004).
27. Valmori, D. *et al.* Enhanced generation of specific tumor-reactive CTL in vitro by selected Melan-A/MART-1 immunodominant peptide analogues. *J Immunol* 160, 1750-1758 (1998).
28. Rivoltini, L. *et al.* A superagonist variant of peptide MART1/Melan A27-35 elicits anti-melanoma CD8+ T cells with enhanced functional characteristics: implication for more effective immunotherapy. *Cancer Res* 59, 301-306 (1999).
29. Ayyoub, M. *et al.* Activation of human melanoma reactive CD8+ T cells by vaccination with an immunogenic peptide analog derived from Melan-A/melanoma antigen recognized by T cells-1. *Clin Cancer Res* 9, 669-677 (2003).
30. Wieckowski, S. *et al.* Fine structural variations of alphabetaTCRs selected by vaccination with natural versus altered self-antigen in melanoma patients. *J Immunol* 183, 5397-5406 (2009).
31. Peixoto, A. *et al.* CD8 single-cell gene coexpression reveals three different effector types present at distinct phases of the immune response. *J Exp Med* 204, 1193-1205 (2007).
32. Messaoudi, I., Guevara Patino, J.A., Dyall, R., LeMaoult, J. & Nikolich-Zugich, J. Direct link between mhc polymorphism, T cell avidity, and diversity in immune defense. *Science* 298, 1797-1800 (2002).
33. Touvrey, C. *et al.* Dominant human CD8 T cell clonotypes persist simultaneously as memory and effector cells in memory phase. *J Immunol* 182, 6718-6726 (2009).
34. Gerlach, C. *et al.* One naive T cell, multiple fates in CD8+ T cell differentiation. *J Exp Med* 207, 1235-1246.
35. Zehn, D., Lee, S.Y. & Bevan, M.J. Complete but curtailed T-cell response to very low-affinity antigen. *Nature* 458, 211-214 (2009).
36. Couedel, C. *et al.* Selection and long-term persistence of reactive CTL clones during an EBV chronic response are determined by avidity, CD8 variable contribution compensating for differences in TCR affinities. *J Immunol* 162, 6351-6358 (1999).
37. Appay, V. *et al.* Memory CD8+ T cells vary in differentiation phenotype in different persistent virus infections. *Nat Med* 8, 379-385 (2002).
38. Rufer, N. *et al.* Ex vivo characterization of human CD8+ T subsets with distinct replicative history and partial effector functions. *Blood* 102, 1779-1787 (2003).
39. Fahmy, T.M., Bieler, J.G., Edidin, M. & Schneck, J.P. Increased TCR avidity after T cell activation: a mechanism for sensing low-density antigen. *Immunity* 14, 135-143 (2001).
40. Cawthon, A.G. & Alexander-Miller, M.A. Optimal colocalization of TCR and CD8 as a novel mechanism for the control of functional avidity. *J Immunol* 169, 3492-3498 (2002).
41. Kersh, E.N. *et al.* TCR signal transduction in antigen-specific memory CD8 T cells. *J Immunol* 170, 5455-5463 (2003).
42. Pittet, M.J. *et al.* High frequencies of naive Melan-A/MART-1-specific CD8(+) T cells in a large proportion of human histocompatibility leukocyte antigen (HLA)-A2 individuals. *J Exp Med* 190, 705-715 (1999).
43. Arden, B., Clark, S.P., Kabelitz, D. & Mak, T.W. Human T-cell receptor variable gene segment families. *Immunogenetics* 42, 455-500 (1995).
44. Romero, P. *et al.* CD8+ T-cell response to NY-ESO-1: relative antigenicity and in vitro immunogenicity of natural and analogue sequences. *Clin Cancer Res* 7, 766s-772s (2001).

Figure 1

A.

Patients	Peptide	# vaccines	Duration (mo)	Persistence (mo)
LAU 205	analog	20	22.4	4.0
LAU 321	analog	8	7.5	10.6
LAU 371	analog	6	6.1	5.0
LAU 444	analog	20	21.9	16.1
LAU 618	analog	12	11.9	11.1
LAU 672	analog	4	2.8	13.4
LAU 818	analog	18	20.5	8.7
LAU 936	analog	7	7	6.0
LAU 944	analog	16	16.3	6.4
LAU 1164	analog	14	36	na
LAU 972	native	20	21.5	6.0
LAU 975	native	4	2.9	2.6
LAU 1013	native	8	8.4	5.6
LAU 1015	native	20	22.4	9.7
LAU 1106	native	27	44.8	7.0

B.

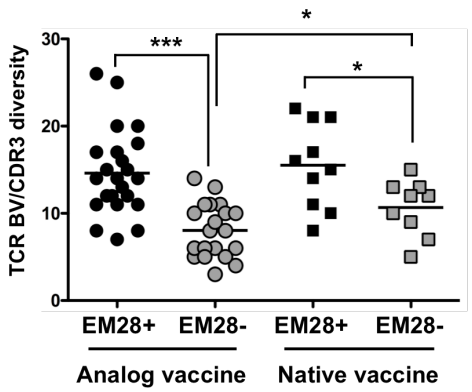

C.

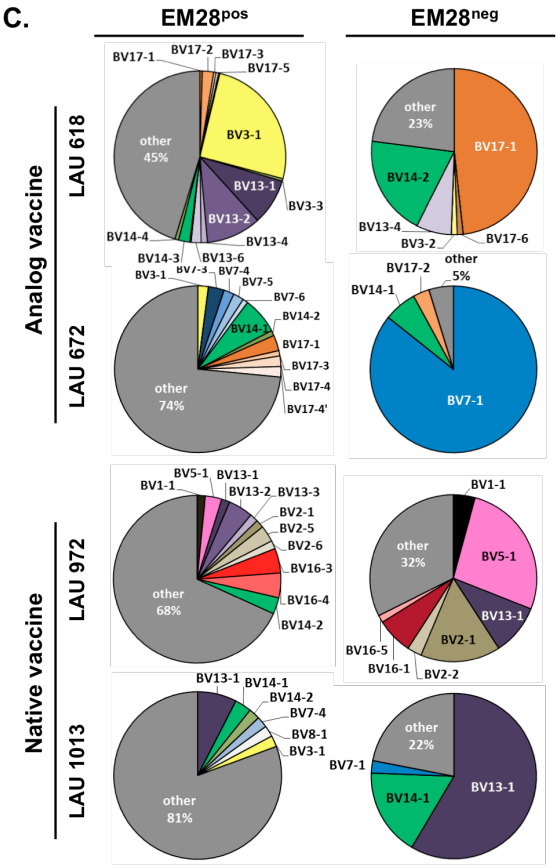

Figure 2

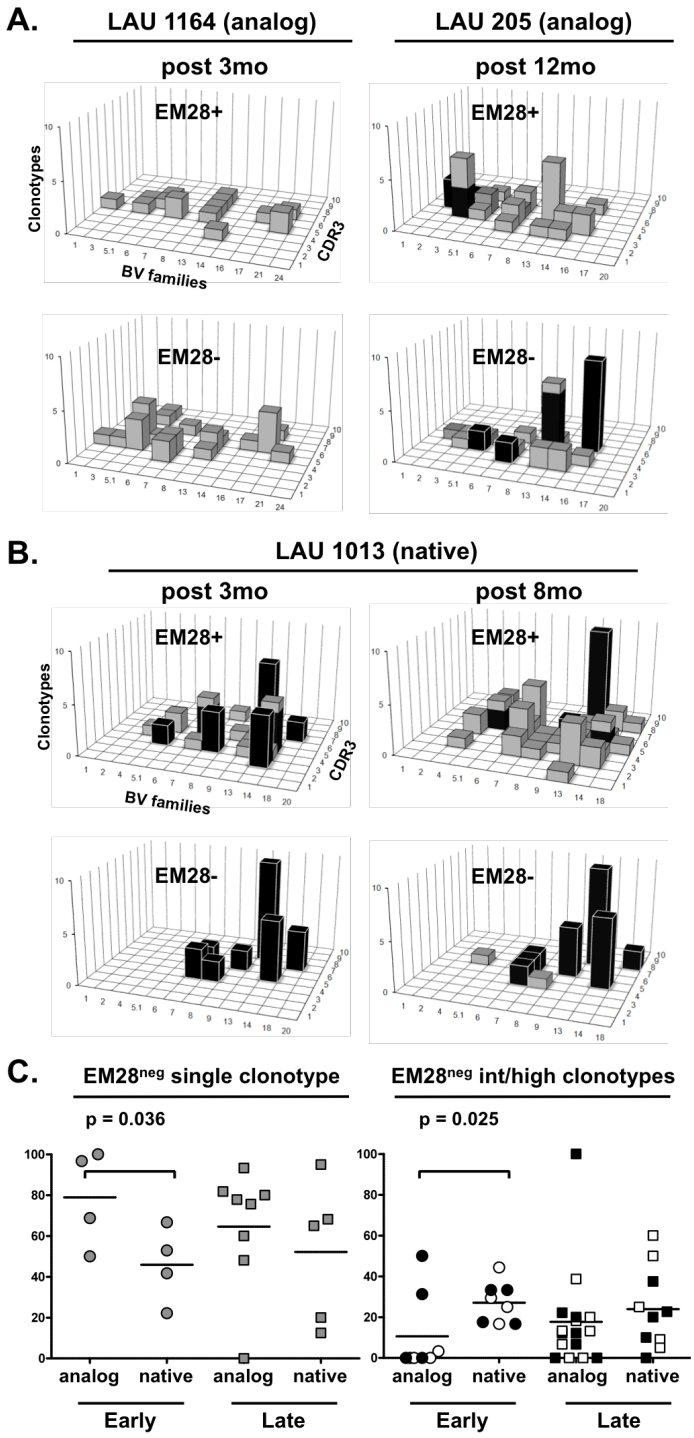
A.
LAU 1164 (analog)
LAU 205 (analog)
post 3mo
post 12mo
EM28+
EM28+
EM28-
EM28-
Clonotypes
BV families
CDR3
B.
LAU 1013 (native)
post 3mo
post 8mo
EM28+
EM28+
EM28-
EM28-
Clonotypes
BV families
CDR3
C.
EM28neg single clonotype
EM28neg int/high clonotypes
p = 0.036
p = 0.025
analog
native
analog
native
Early
Late
analog
native
analog
native
Early
Late

Figure 3

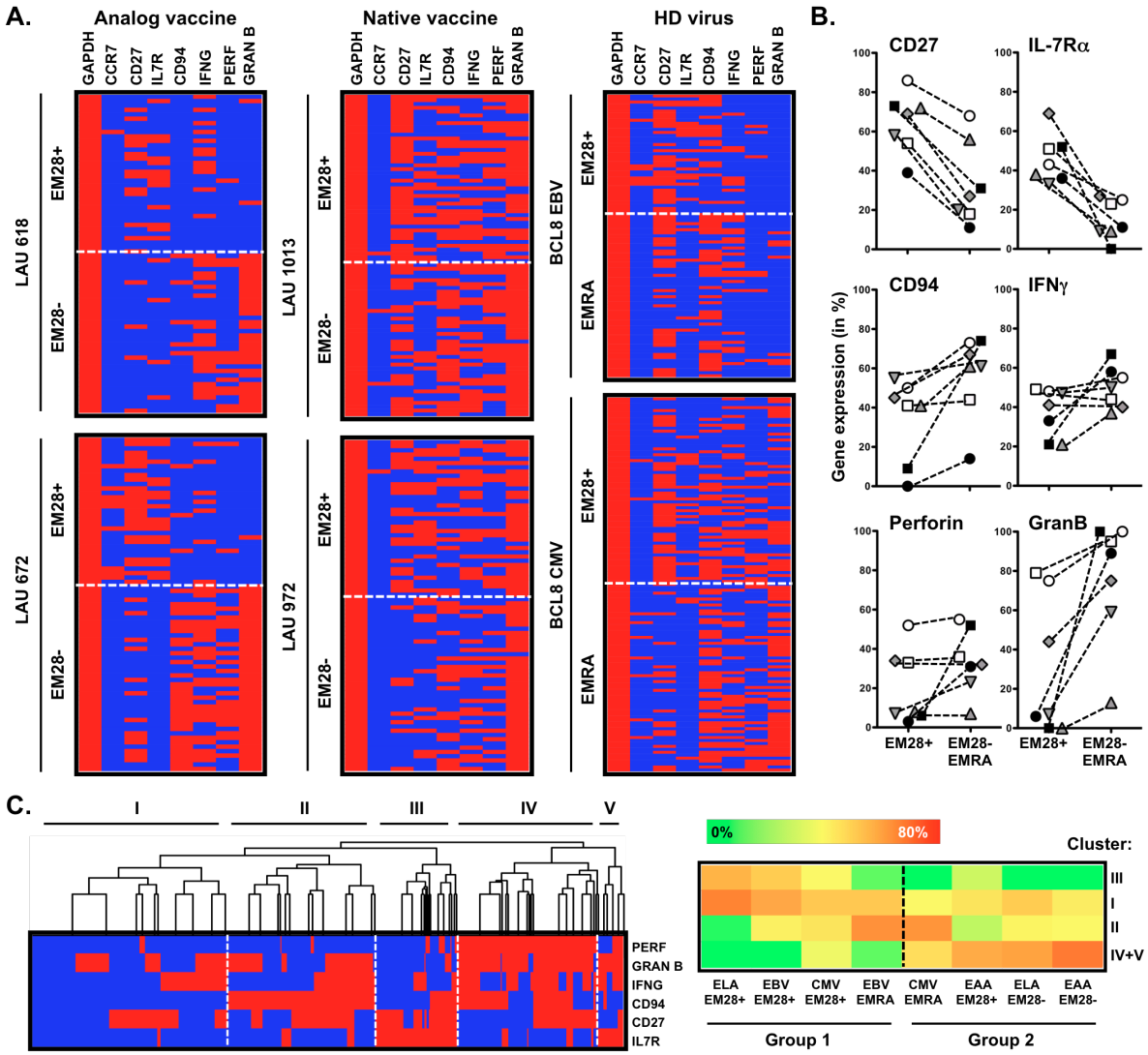
A.
Analog vaccine
Native vaccine
HD virus
GAPDH
CCR7
CD27
IL7R
CD94
IFNG
PERF
GRAN B
LAU 618
LAU 1013
LAU 672
LAU 972
BCL8 EBV
BCL8 CMV
EM28+
EM28-
EMRA
B.
CD27
IL-7Rα
CD94
IFNγ
Perforin
GranB
Gene expression (in %)
EM28+
EM28-
EMRA
C.
I
II
III
IV
V
PERF
GRAN B
IFNG
CD94
CD27
IL7R
0%
80%
Cluster:
III
I
II
IV+V
ELA EM28+
EBV EM28+
CMV EM28+
EBV EMRA
CMV EMRA
EAA EM28+
ELA EM28-
EAA EM28-
Group 1
Group 2

Figure 4

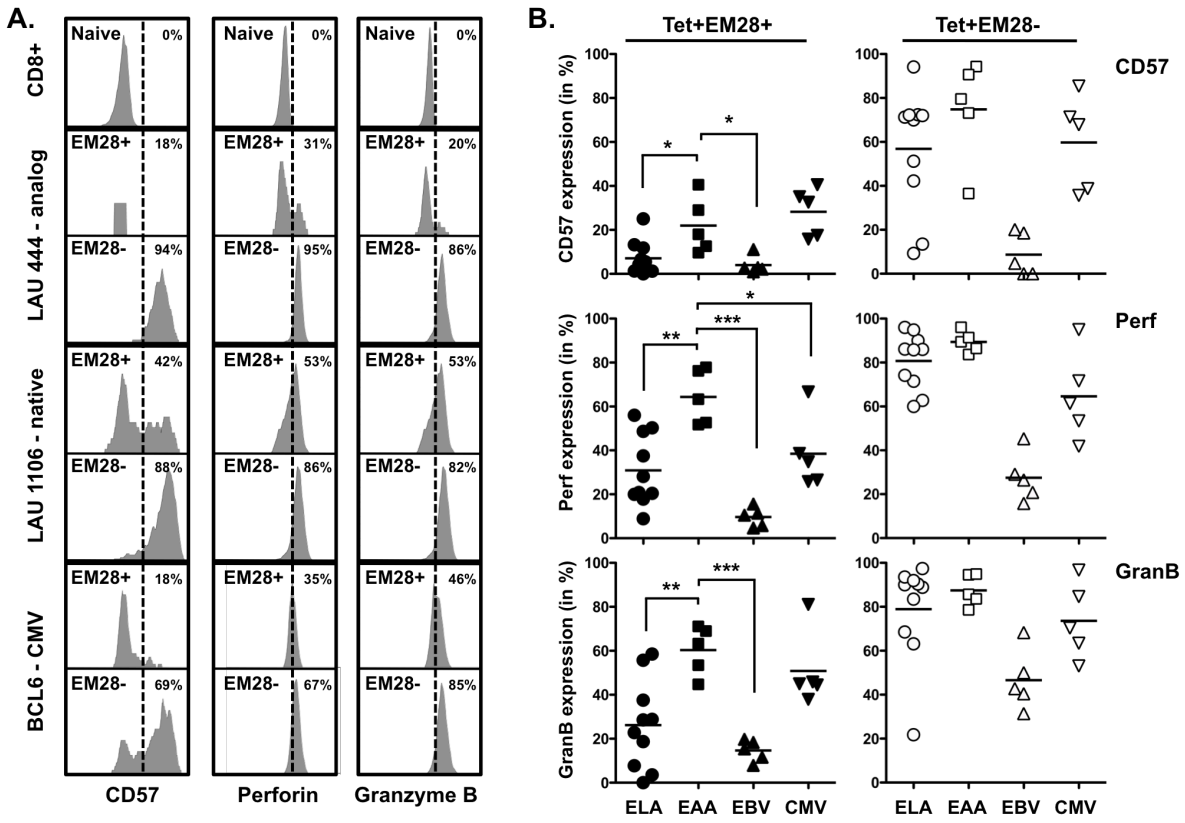
A.
CD8+
LAU 444 - analog
LAU 1106 - native
BCL6 - CMV
Naive
0%
EM28+
18%
EM28-
94%
EM28+
42%
EM28-
88%
EM28+
18%
EM28-
69%
Naive
0%
EM28+
31%
EM28-
95%
EM28+
53%
EM28-
86%
EM28+
35%
EM28-
67%
Naive
0%
EM28+
20%
EM28-
86%
EM28+
53%
EM28-
82%
EM28+
46%
EM28-
85%
CD57
Perforin
Granzyme B
B.
Tet+EM28+
Tet+EM28-
CD57
Perf
GranB
CD57 expression (in %)
Perf expression (in %)
GranB expression (in %)
ELA
EAA
EBV
CMV

Figure 5

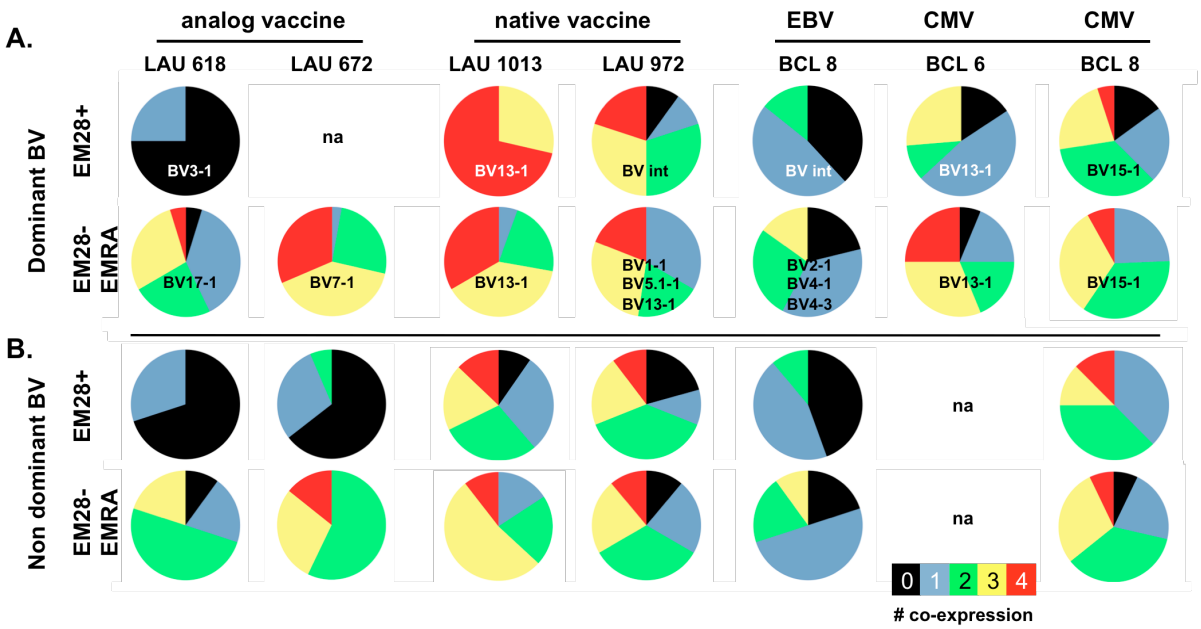
A.
analog vaccine
native vaccine
EBV
CMV
CMV
LAU 618
LAU 672
LAU 1013
LAU 972
BCL 8
BCL 6
BCL 8
Dominant BV
EM28+
EM28-
EMRA
BV3-1
na
BV13-1
BV int
BV int
BV13-1
BV15-1
BV17-1
BV7-1
BV13-1
BV1-1
BV5.1-1
BV13-1
BV2-1
BV4-1
BV4-3
BV13-1
BV15-1
B.
Non dominant BV
EM28+
EM28-
EMRA
na
na
0 1 2 3 4
co-expression

Figure 6

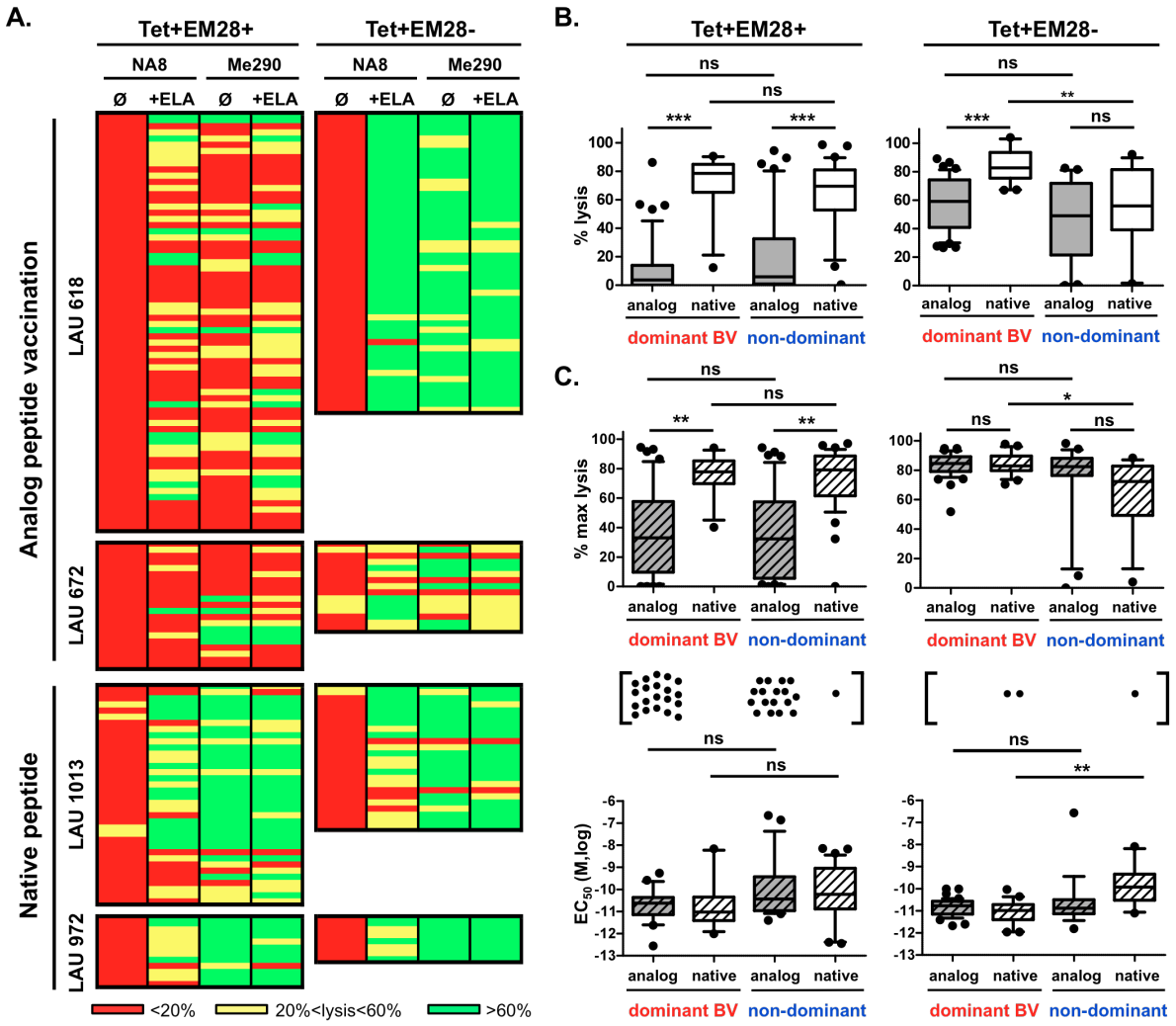
A.
Tet+EM28+
Tet+EM28-
NA8
Me290
Ø
+ELA
Analog peptide vaccination
Native peptide
LAU 618
LAU 672
LAU 1013
LAU 972
<20%
20%<lysis<60%
>60%
B.
% lysis
C.
% max lysis
EC50 (M,log)
analog
native
dominant BV
non-dominant
ns
*
**
***

Figure 7

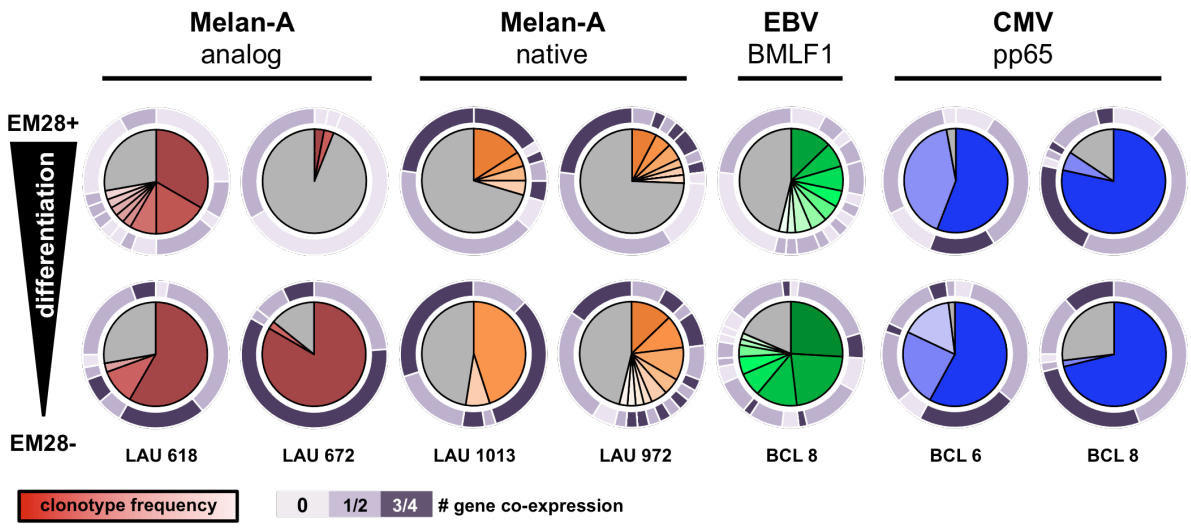
Melan-A
analog
Melan-A
native
EBV
BMLF1
CMV
pp65
EM28+
differentiation
EM28-
LAU 618
LAU 672
LAU 1013
LAU 972
BCL 8
BCL 6
BCL 8
clonotype frequency
0
1/2
3/4
gene co-expression

SUPPORTING INFORMATION

Supplemental Table 1. Clinical characteristics of patients

Patient	Gender	Age at diagnosis (years)	Disease stage at diagnosis	Type of vaccine[1]	# of vacci-nations	Duration[2] (mo)	Clinical outcome
LAU 205	M	24	pT2aN1M0	ELA+IFA+CpG	20	22.4	†
LAU 321	M	60	pT3aN0M0,IIa	ELA+IFA+CpG	8	7.5	
LAU 371	F	30	pT3aN1M0,III	ELA+IFA+CpG	6	6.1	†
LAU 444	F	28	pT3aN0M0	ELA+IFA+CpG	20	21.9	†
LAU 618	F	70	pT4N0M0	ELA+IFA+CpG	12	11.9	
LAU 672	M	35	pT1N0M0	ELA+IFA+CpG	4	2.8	†
LAU 818	M	55	pT3bN0M0,IIb	ELA+IFA+CpG	18	20.5	
LAU 936	F	52	pT3aN0M0,IIa	ELA+IFA+CpG	7	7.0	†
LAU 944	F	20	pT1aN0M0	ELA+IFA+CpG	16	16.3	
LAU 1164	M	52	pTxNxM1a	ELA+IFA+CpG	14	36.0	
LAU 972	F	60	pT2bN1M0	EAA+IFA+CpG	20	21.5	
LAU 975	M	52	pT4N1bM0	EAA+IFA+CpG	4	2.9	†
LAU 1013	M	56	pT3bN3M0	EAA+IFA+CpG	8	8.4	†
LAU 1015	M	75	pT2aN0M1a,IV	EAA+IFA+CpG	20	22.4	†
LAU 1106	M	36	pT2aN1M0,IIIa	EAA+IFA+CpG	27	44.8	

[1] ELA refers to the analog peptide and EAA to the native unmodified peptide
[2] Time (months) during which the patient received monthly vaccinations

SUPPLEMENTAL FIGURE LEGENDS

Supplemental Figure 1. *Ex vivo* analysis of circulating Melan-A^{MART-1} 26-35 specific CD8 T-cells over time in melanoma patients vaccinated with either the analog A27L-modified (*A*; n = 10) or the unmodified native (*B*; n = 5) peptide, combined with CpG and IFA. *A* and *B*, Percentages of CD28^{pos} (empty bars) and CD28^{neg} (filled bars) Melan-A^{MART-1}-specific T-cells in CD8^{pos} T-cells from peripheral blood was measured by flow cytometry at the indicated time-points before (defined as time 0) and after vaccination, using CD8- and CD28-specific Abs and HLA-A2/Melan-A^{MART-1} multimers. For patients LAU 371, LAU 936, and LAU 1013, the proportion of multimer^{pos} T cells was below ≤ 0.02% before the start of peptide vaccination. Vaccinations are indicated by filled circles.

Supplemental Figure 2. TCR BV diversity analysis and quantification of Melan-A-specific T-cell clonotypes. *A*, cDNA pools (50 cells) generated from *ex vivo* EM28^{pos} and EM28^{neg} tumor-reactive T-cells sorted from blood of patients vaccinated with analog (LAU 618 and LAU 672) or native (LAU 972 and LAU 975) peptide were amplified by PCR using 22 BV-specific primers and subjected to electrophoresis. Each BV subfamily (x-axis) was analyzed for the presence of amplified BV-CDR3-BC products of defined CDR3 size (y-axis), and displayed by black squares on a grid. The figures inserted in each grid indicate the # of TCR BV subfamily usage versus the # of all amplified BV-CDR3-BC products. *B*, Clonotypic PCR was performed on *in vitro* generated specific T-cell clones from patients vaccinated either with analog (LAU 936, n = 91; LAU 1164, n = 120) or native peptide (LAU 1015, n = 204; LAU 1106, n = 130). Time-points after start of vaccination were 7 mo (LAU 936), 1 mo (LAU 1164), 13 mo (LAU 1015) and 8 mo (LAU 1106), respectively. Each clonotype with a frequency ≥ 1% is indicated. Non-dominant clonotypes are designed as "BV other" and are comprised of clonotypes of unique TCR BV/CDR3 sizes and/or BV-CDR3-BC sequences as determined by capillary electrophoresis and sequencing. *C*, Repartition of dominant and non-dominant T-cell clonotypes within EM28^{pos} and EM28^{neg} T-cell subsets and within antigenic specificities (analog/ELA or native/EAA tumor antigens, EBV or CMV epitopes). Dominant clonotypes are defined as high (≥ 10 %, in blue) or intermediate (1-9 %, green) frequency. The proportion of non-dominant clonotypes (< 1%) is depicted in grey. Mo, months.

Supplemental Figure 3. Analysis of T-cell clonotype diversity and frequency in circulating Melan-A-specific T-cell subsets over time. TCR BV spectratyping was performed on cDNA

obtained from individually sorted 5-cell samples of specific EM28^{pos} and EM28^{neg} CD8 T cells from patients after vaccination with analog (n = 9) or native peptide (n = 5). *A*, Complete data representing the proportions of single non dominant (*left panel*) and dominant (*right panel*) clonotypes identified in the EM28^{pos} subset of the indicated patient cohort and time-point after vaccination. Early time-point, 1 to 3 months; late time-point, > 3 months. Dominant TCR clonotypes are defined as identical BV-CDR3-BC sequences found at least twice and non-dominant single TCR clonotypes are defined by their unique TCR BV/CDR3 size length and/or BV-CDR3-BC sequence. Dominant clonotypes were further classified according to their relative frequencies among tumor-specific EM28^{pos} subsets as high frequency (i.e. > 25%; empty symbols) and intermediate frequency (i.e. 1-25%, filled symbols). *P*-values were calculated with the two-tailed unpaired *t* test. *B*, Collection of dominant T-cell clonotypes shared between EM28^{pos} and EM28^{neg} subsets of patients vaccinated with analog (ELA) or native (EAA) peptide. For each clonotype, we indicate the type of peptide vaccination, the patient code, the time-point tested after vaccination, and its frequency within EM28^{pos} and EM28^{neg} subsets.

Supplemental Figure 4. *Ex vivo* gene expression analysis of effector mediators in Melan-A-specific CD8 T-cell subsets at the single-cell level. *A*, Examples of gene expression profiles in two patients vaccinated with the analog peptide (LAU 672) or the native peptide (LAU 972). Primers designed for GAPDH, CCR7, CD27, IL-7Rα, CD94, IFN-γ, perforin and granzyme B mRNA transcripts are depicted. Data from 15 independent single-cell aliquots are shown. *B*, The pie charts depict co-expression profiles of *CD94*, *IFN-γ*, *perforin* and *granzyme B* within the single-cell samples of tumor- and virus-specific EM28^{pos} and EM28^{neg}/EMRA T-cell subsets.

Supplemental Figure 5. *Ex vivo* analysis of expression of effector proteins in Melan-A-specific CD8 T-cell subsets by multi-parameter flow cytometry. *A*, The proportion of CD27, IL-7Rα and PD1 protein expression was determined within EM28^{pos} and EM28^{neg} T-cell subsets from melanoma patients following analog (ELA, n = 10) or native (EAA, n= 5) peptide vaccination, and from healthy individuals with EBV (n= 5) and/or CMV (n = 5) specific T-cells. B, Flow cytometry analysis of CD27, IL-7Rα, PD1, CD57, perforin and granzyme B expression was performed on bulk EM28^{pos} and EM28^{neg} CD8 T cells from the same tested samples as depicted in *A*, and Fig. 4, providing internal staining control.

Supplemental Figure 6. Tumor cell killing and efficiency of antigen recognition. Tumor-specific T-cell clones were generated *in vitro* by limiting-dilution from blood samples corresponding to the same time-points after vaccination as those depicted in Fig. 1C. *A*, Complete data representing specific lysis of the Melan-A^+ Me 290 tumor cell line in the absence of exogenous Melan-A peptide (10:1; effector:target ratio) by T-cell clones derived from $EM28^{pos}$ and $EM28^{neg}$ cells of patients vaccinated with analog peptide (grey whiskers) or native peptide (empty whiskers). *B*, The relative TCR avidity was compared using T2 target cells ($A2^+/TAP^{-/-}$) pulsed with graded concentrations of either analog (ELA) or native (EAA) Melan-A_{26-35} peptide. Complete data representing maximal lysis (*upper panel*) and EC_{50} (e.g. peptide concentration required to achieve 50% of maximal lysis; *lower panel*). Clones with undetectable lytic activity ($EC_{50} > 10^{-6}$ M and/or maximal lysis < 20%) are symbolized as single dots above the y-axis to visualize them in the figures, and were not included in the statistical evaluations. * $0.01 < P < 0.001$, ** $0.001 < P < 0.0001$, *** $P < 0.0001$ (two-tailed unpaired *t* test).

SUPPLEMENTAL METHODS

Patients

HLA-A2-positive patients with histological proven metastatic (stage III/IV) melanoma expressing Melan-A (RT-PCR or immuno-histochemistry) were included upon written informed consent, as described previously (1, 2). The following inclusion criteria had to be fulfilled: Karnofsky performance status of 70%, normal CBC and kidney-liver function, no concomitant anti-tumor therapy nor immunosuppressive drugs. Exclusion criteria were pregnancy, seropositivity for HIV-1 Ab or HBs Ag, brain metastases, uncontrolled bleeding, clinically significant autoimmune disease, and symptomatic heart disease (NYHA III-IV). Study end points were toxicity and CD8 T cell responses.

Antibodies

Extracellular and intracellular stainings were performed according to the manufacturer's instructions. All FACS sorting experiments (*ex vivo* 5-cell and single-cell aliquots, and *in vitro* generation of T-cell clones) were performed using the following 5-color stain combination: (1) PE-HLA-A2/peptide multimers, (2) FITC-conjugated anti-CD28 (BD Pharmingen), (3) PE-Texas Red-conjugated anti-CD45RA (Beckman Coulter), (4) APC-Cy7-conjugated anti-CD8 (BD Pharmingen) reagents and (5) anti-CCR7 mAb (BD Pharmingen) followed by APC-conjugated goat anti-rat IgG Ab (for indirect staining for CCR7) (Caltag Laboratories).

Multi-parameter flow cytometry analyses were performed using the following 8-color stain strategy: (1) PE-HLA-A2/peptide multimers, (2) FITC-conjugated anti-CD57 (BD Pharmingen) or -PD1 (BD Pharmingen) or -Granzyme B (Hölzer Diagnostic) or –Perforin (Ancell), (3) PE-Texas Red-conjugated anti-CD45RA (Beckman Coulter), (4) PE-Cy7-conjugated CCR7 (BD Pharmingen), (5) Alexafluor700 anti-CD28 (Biolegend), (6) Pacific Blue-labeled anti-CD8, (7) PerCP-Cy5.5 anti-CD127 (IL-7R) (Beckman Coulter), and (8) APC-eFluor780-conjugated anti-CD27 (eBioscience) mAbs.

Direct cell lysis and cDNA synthesis

Single-cell or five-cell aliquots were sorted by flow cytometry directly into 96-V bottom plates containing 15 μl of a lysis/cDNA mix solution supplemented with 1.2% Triton X-100

(Fluka), 30 μg/ml tRNA (Roche), 10 mM DTT (Fluka), 0.5 mM dNTP (Invitrogen, Paisley, UK), 2 ng/μl of a 20-mer oligo-dT (Amplimmun, Madulain, Switzerland), 4 U of RNAsin (Promega, Madison, WI), 3 μl of RT buffer (5x; Invitrogen) and 40 U of M-MLV transcriptase (Invitrogen), as described in detail elsewhere (1). To allow the transcription of total mRNA into cDNA, the 96-well plates were incubated 60 min at 37°C and briefly centrifuged and transferred into 0.5 ml PCR tubes. MMLV-RT transcriptase was inactivated at 90°C for 3 min and samples were stored at -80°C until further use. For T cell clones, 15 μl of lysis/cDNA mix was directly added to 10^5 cells and further processed as described above.

Global cDNA amplification from single-cells

The basic principle of the five-cell and single-cell global cDNA amplification protocol requires that the target sequences to be amplified be flanked by known sequences to which the amplification primers can anneal and initiate polymerization. One end is initially defined through a cDNA reaction using reverse transcriptase and an oligo(dT) primer that will prime via the poly(A) tail present at the 3' end of most mRNA molecules. The other end is then created by the addition of an homopolymer d(A) sequence to the 3'-OH end of the first cDNA using terminal deoxynucleotidyl transferase. Global PCR amplification of the dA/dT flanked cDNAs is carried out using a single modified oligo(dT) primer as previously described by Brady and Iscove (4). Priming of the cDNA during global RT-PCR is initiated via annealing of the d(T) region of the 61-mer oligonucleotide primer to the homopolymeric d(A) regions present at the termini of the cDNA molecules. We have included a purification step before adding the poly d(A) tails, in order to get rid of free dNTPs that may interfere during the tailing reaction. Therefore, for further processing, cDNA from single-cell or five-cell aliquots were precipitated overnight at -20°C after addition of 7.5 μl of $C_2H_7NO_2$ 7.5 M (Fluka), 45 μl of ethanol 100% (Fluka) using 2 μl of Glycogen 10 mM (Roche) as carrier, washed in 150 μl of cold ethanol 70% and dried 1 hour at room temperature.

To evaluate mRNA expression in small numbers of cells (1-10 cells), the following method was adapted from previously published protocols (4, 5). Briefly, to allow 3'oligo(dA) tailing to cDNA, the dried pellets were suspended in 5 μl of tailing solution containing 0.5 mM dATP (Amersham Pharmacia), 1 U of Terminal deoxynucleotidyl Transferase (Promega) and 1 μl tailing buffer (5x; Promega) and incubated at 37°C for 30 min. After denaturation (94°C for 3 min), 45 μl of PCR-buffer (10 mM TRIS-HCl pH 8.8, 50 mM KCl, 0.1 mg/ml BSA, 2

mM $MgCl_2$) containing 20 ng/µl of a 61-mer oligo dT (5'-CATGTCGTCCAGGCCGCTCTG GGACAAAATATGAATTCT$_{23}$-3') (Metabion), 0.2 mM dNTP, 0.5% Triton X-100, and 5 U Taq DNA recombinant polymerase Platinum (Invitrogen) were added, followed by 5 cycles of PCR (50s at 94°C; 2 min at 37°C; 9 min at 72°C) and of 35 cycles (50s at 94°C; 90s at 60°C; 8 min at 72°C). 1 µl of amplified cDNA (also defined as $cDNA^{plus}$) was then subjected to a second round of PCR amplification (38-40 cycles, 30s at 94°C; 45s at 58°C; 1 min at 72°C) in 20 µl volumes of 1x PCR buffer containing 1.5 mM $MgCl_2$, 0.2 mM dNTP, 0.5 U Taq Platinum and 40 ng of specific primers designed to amplify mRNA sequences of interest and the expected products were visualized after electrophoresis on a 1.2% agarose gel. Typically, we used H_20 for the negative PCR control, while 10^3 PBMCs from a healthy individual was used as positive PCR control.

Gene expression analysis

For gene expression analysis of single cells, we used the following primers: *CD3*: 5'-CGTTCAGTTCCCTCCTTTTCTT-3'; rev-5'-GATTAGGGGGTTGGTAGGGAGTG-3', *GAPDH*: 5'- GGACCTGACCTGCCGTCTAG-3'; rev-5'-CCACCACCCTGTTGCTGTAG-3', *CCR7*: 5'-CCAGGCCTTATCTCCAAGACC-3'; rev-5'-GCATGTCATCCCCACTCTG-3', *CD27*: 5'-ACGTGACAGAGTGCCTTTTCG-3'; rev-5'-TTTGCCCGTCTTGTAGCATG-3', *CD127/IL-7Ra*: 5'-ATCTTGGCCTGTGTGTTATGG-3'; rev-5'-ATTCTTCTAGTTGCT GAGGAAACG-3'; *CD94*: 5'-GTGGGAGAATGGCTCTGCAC -3'; rev-5'-TGAGCTGTT GCTTACAGATATAACGA-3', *IFN-γ*: 5'-GCCAACCTAAGCAAGATCCCA-3'; rev-5'-GGAAGCACCAGGCATGAAATC-3', *Perforin*: 5'-TTCACTGCCACGGATGCCTAT-3'; rev-5'-GCGGAATTTTAGGTGGCCA-3', *Granz B*: 5'-GCAGGAAGATCGAAAGTGCGA-3'; rev-5'-GCATGCCATTGTTTCGTCCAT-3'.

TCR spectratyping, sequencing and clonotyping

To rapidly identify TCR Vβ segment usage, a small fraction (5 µl of a total of 50 µl) from 10 individually sorted and amplified 5-cell cDNA samples were pooled and subjected to individual PCR in non-saturating conditions using a set of previously validated fluorescent-labeled forward primers specific for the 22 TCR Vβ subfamilies and one unlabeled reverse primer specific for the corresponding C gene segment (6, 7). This TCR Vβ-CDR3 spectratyping analysis based on the equivalent of 50 cells represents a pre-screening step.

Once positive TCR Vβ subfamilies were identified, the following step consisted in subjecting each individually generated single-cell or 5-cell cDNA sample, and in parallel *in vitro* generated T cell clone to TCR Vβ PCRs. Separation and detection of amplified fragments that contain the entire CDR3 segment was performed in the presence of fluorescent size markers on an ABI PRISM 310 Genetic Analyzer (AppliedBiosystems, Rotkreuz, Switzerland) according to the manufacturer's recommendations, and data were analyzed with GeneScan 3.7.1 (AppliedBiosystems). In the last step, PCR products of interest were directly purified and sequenced from the reverse primer (Fasteris SA, Plan-les-Ouates, Switzerland). Clonotypic primers for several CDR3 sequences were validated and used in clonotypic PCR for determination of clonotype frequencies (*unpublished data*).

REFERENCES

1. Speiser, D. E., D. Lienard, N. Rufer, V. Rubio-Godoy, D. Rimoldi, F. Lejeune, A. M. Krieg, J. C. Cerottini, and P. Romero. 2005. Rapid and strong human CD8+ T cell responses to vaccination with peptide, IFA, and CpG oligodeoxynucleotide 7909. *J Clin Invest* 115:739-746.
2. Speiser, D. E., P. Baumgaertner, V. Voelter, E. Devevre, C. Barbey, N. Rufer, and P. Romero. 2008. Unmodified self antigen triggers human CD8 T cells with stronger tumor reactivity than altered antigen. *Proc Natl Acad Sci U S A* 105:3849-3854.
3. Rufer, N., P. Reichenbach, and P. Romero. 2005. Methods for the ex vivo characterization of human CD8+ T subsets based on gene expression and replicative history analysis. *Methods Mol Med* 109:265-284.
4. Brady, G., and N. N. Iscove. 1993. Construction of cDNA libraries from single cells. *Methods Enzymol* 225:611-623.
5. Sauvageau, G., P. M. Lansdorp, C. J. Eaves, D. E. Hogge, W. H. Dragowska, D. S. Reid, C. Largman, H. J. Lawrence, and R. K. Humphries. 1994. Differential expression of homeobox genes in functionally distinct CD34+ subpopulations of human bone marrow cells. *Proc Natl Acad Sci U S A* 91:12223-12227.
6. Roux, E., C. Helg, F. Dumont-Girard, B. Chapuis, M. Jeannet, and E. Roosnek. 1996. Analysis of T-cell repopulation after allogeneic bone marrow transplantation: significant differences between recipients of T-cell depleted and unmanipulated grafts. *Blood* 87:3984-3992.
7. Roux, E., F. Dumont-Girard, M. Starobinski, C. A. Siegrist, C. Helg, B. Chapuis, and E. Roosnek. 2000. Recovery of immune reactivity after T-cell-depleted bone marrow transplantation depends on thymic activity. *Blood* 96:2299-2303.

Supplemental Figure 1

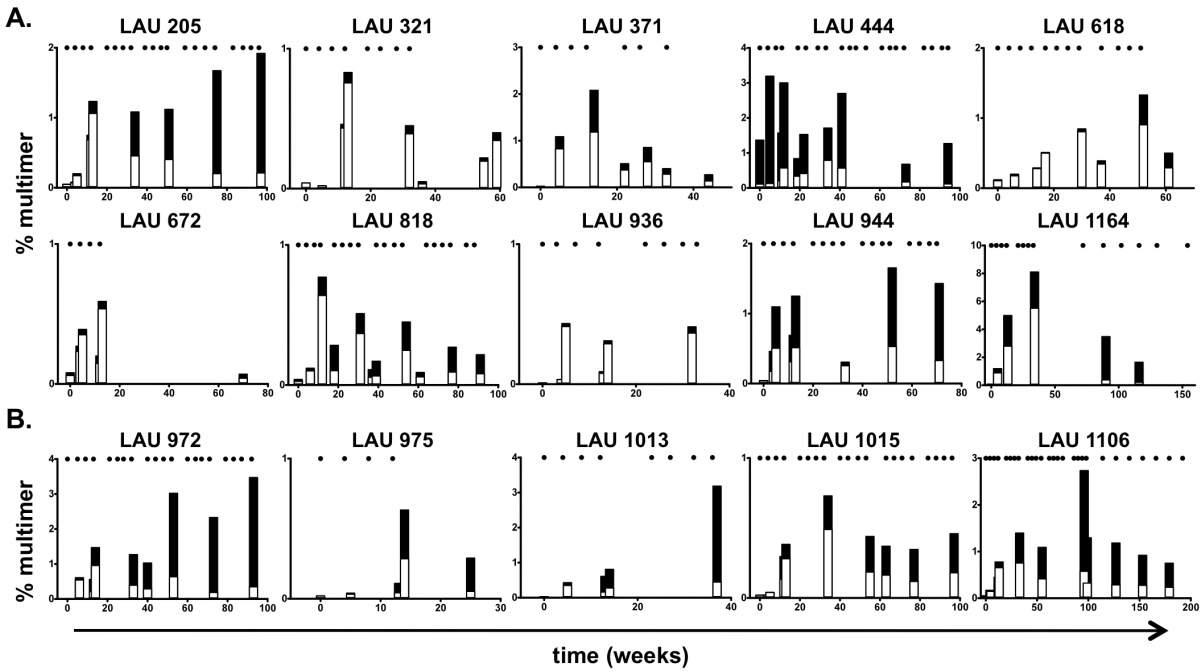

Supplemental Figure 2

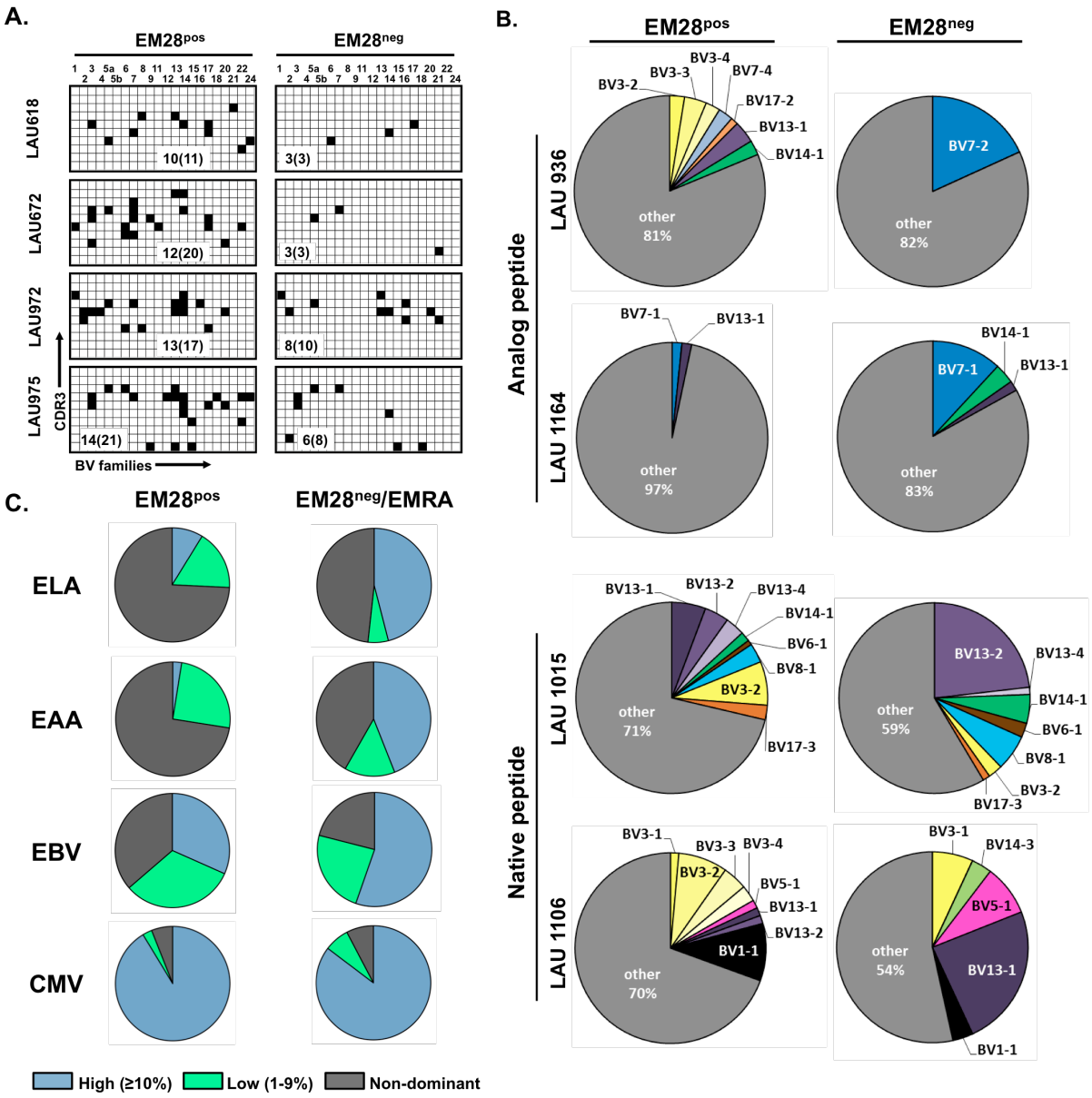

Supplemental Figure 3

A.

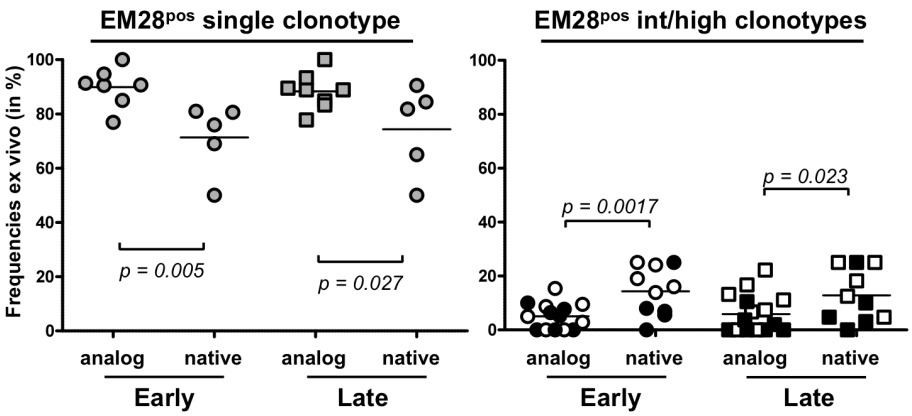

B.

Cohort	Patient	Clonotype	Time	EM28+	EM28-
Analog peptide	LAU 205	BV16-1	+ 8 mo	**5/15**	**8/15**
	LAU 618	BV17-1	+ 12 mo	**10/15**	**14/15**
	LAU 627	BV3-1	+ 3 mo	**5/16**	2/14
		BV12-1	+ 3 mo	**4/16**	2/14
	LAU 672	BV14-1	+ 3 mo	**3/8**	**4/8**
	LAU 818	BV3-1	+ 12 mo	**4/15**	2/13
	LAU 944	BV24-1	+ 1 mo	**10/20**	**18/20**
		BV24-1	+ 3 mo	**4/15**	**13/13**
		BV24-1	+ 8 mo	**4/19**	**20/20**
Native peptide	LAU 972	BV1-1	+ 3 mo	**6/15**	**7/15**
		BV1-1	+ 9 mo	2/12	**8/15**
		BV2-1	+ 9 mo	2/12	2/15
		BV13-1	+ 3 mo	**7/15**	**7/15**
		BV13-1	+ 9 mo	2/12	**9/15**
	LAU 975	BV3-1	+ 3 mo	**10/20**	**19/20**
		BV3-2	+ 3 mo	**19/20**	**12/20**
		BV3-2	+ 6 mo	**8/8**	**9/19**
		BV3-3	+ 3 mo	**11/20**	**7/20**
		BV5-1	+ 3 mo	4/20	**6/20**
		BV7-1	+ 3 mo	3/20	3/20
		BV14-1	+ 3 mo	2/20	3/20
	LAU 1013	BV7-1	+ 8 mo	2/15	2/15
		BV7-3	+ 8 mo	3/15	3/15
		BV8-1	+ 3 mo	4/15	2/15
		BV13-1	+ 3 mo	**7/15**	**10/15**
		BV13-1	+ 8 mo	**9/15**	**13/15**
		BV14-1	+ 3 mo	2/15	**6/15**
		BV14-1	+ 8 mo	2/15	**7/15**
		BV18-1	+ 3 mo	2/15	4/15
		BV9-1	+ 8 mo	2/15	**5/15**
	LAU 1015	BV3-1	+ 3 mo	**3/15**	**11/14**
		BV4-1	+ 3 mo	**4/15**	**7/14**
		BV6-1	+ 3 mo	3/15	3/14
		BV6-2	+ 13 mo	2/15	2/12
		BV7-1	+ 3 mo	2/15	2/15
		BV8-1	+ 3 mo	**11/15**	**9/14**
		BV14-1	+ 3 mo	3/15	4/14
		BV16-1	+ 3 mo	3/15	2/14

Supplemental Figure 4

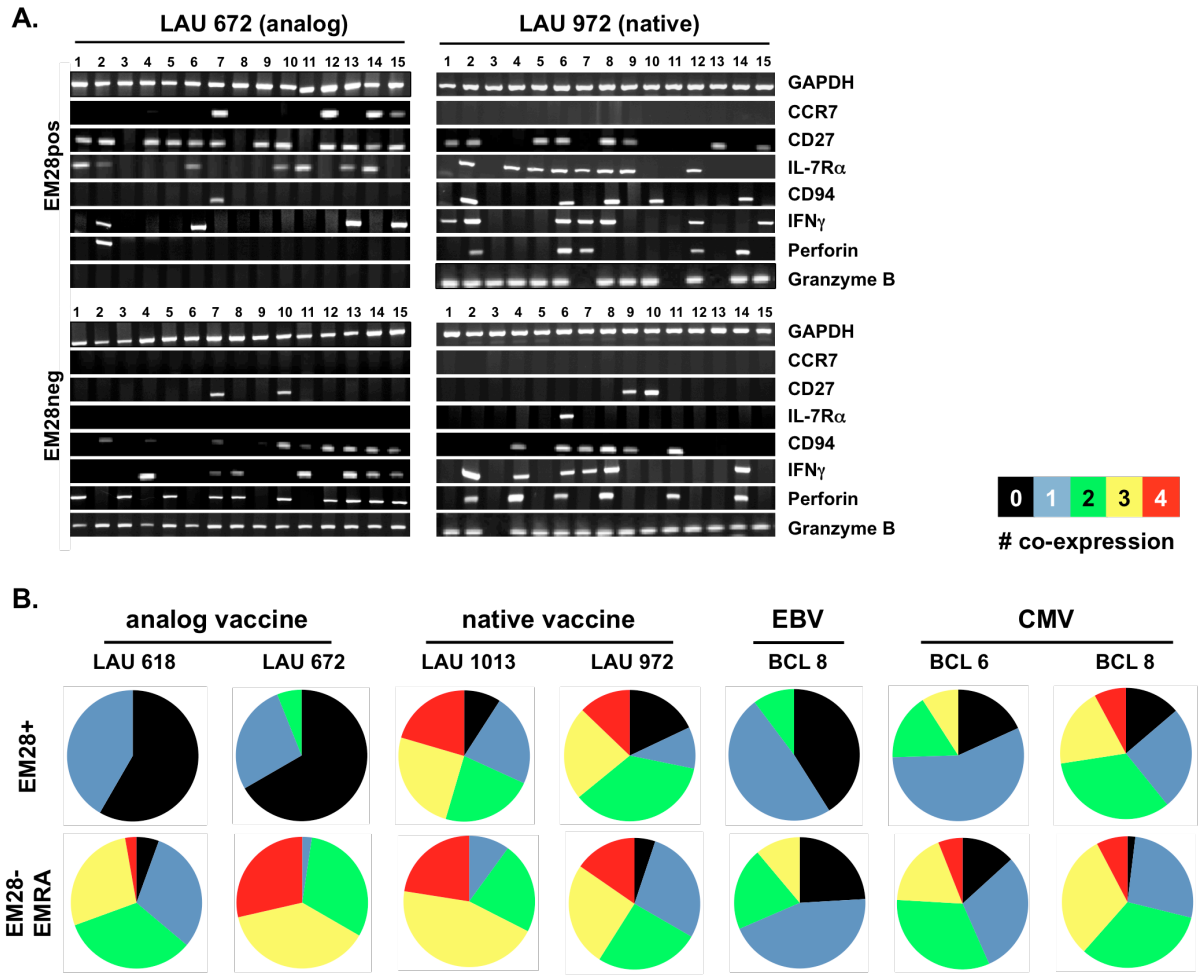

Supplemental Figure 5

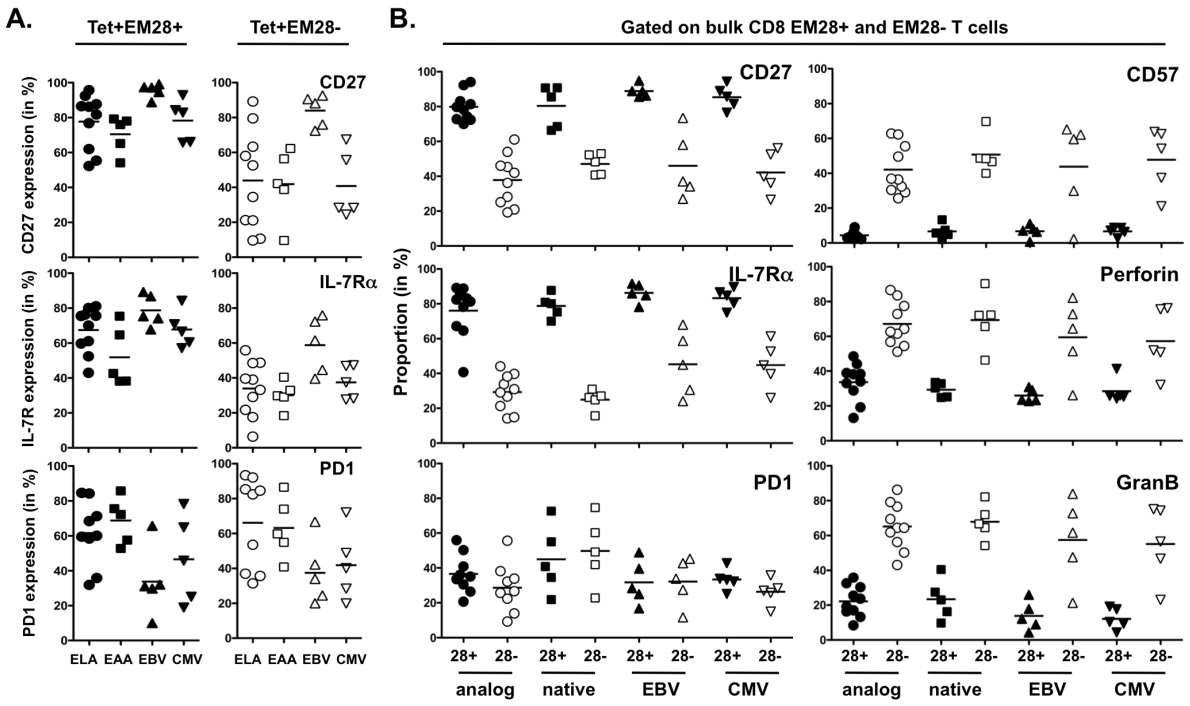

Supplemental Figure 6